

EPA/600/R-94/018
February 1994

**ABIOTIC TRANSFORMATION OF CARBON TETRACHLORIDE
AT MINERAL SURFACES**

by


Michelle Kriegman-King and Martin Reinhard
Department of Civil Engineering
Stanford University
Stanford, California 94305-4020

CR-816776

Project Officer

Stephen R. Hutchins
Processes and Systems Research Division
Robert S. Kerr Environmental Research Laboratory
Ada, Oklahoma 74820

ROBERT S. KERR ENVIRONMENTAL RESEARCH LABORATORY
OFFICE OF RESEARCH AND DEVELOPMENT
U.S. ENVIRONMENTAL PROTECTION AGENCY
ADA, OKLAHOMA 74820

TECHNICAL REPORT DATA <i>(Please read Instructions on the reverse before completing)</i>		
1. REPORT NO.	2.	3.  PB94-144698
4. TITLE AND SUBTITLE ABIOTIC TRANSFORMATION OF CARBON TETRACHLORIDE AT MINERAL SURFACES	5. REPORT DATE February 1994	
	6. PERFORMING ORGANIZATION CODE	
7. AUTHOR(S) Michelle Kriegman-King and Martin Reinhard	8. PERFORMING ORGANIZATION REPORT NO.	
9. PERFORMING ORGANIZATION NAME AND ADDRESS Department of Civil Engineering Stanford University Stanford, CA 94301-4020	10. PROGRAM ELEMENT NO. AC4C1A	
	11. CONTRACT/GRANT NO. CR-816776	
12. SPONSORING AGENCY NAME AND ADDRESS Robert S. Kerr Environmental Research Lab. - Ada, OK U.S. EPA P.O. Box 1198 Ada, OK 74820	13. TYPE OF REPORT AND PERIOD COVERED Final Report 09/90 - 09/93	
	14. SPONSORING AGENCY CODE EPA/600/15	
15. SUPPLEMENTARY NOTES Project Officer: Stephen R. Hutchins 405/436-8563		
16. ABSTRACT <p>Transformation of carbon tetrachloride (CCl₄) by biotite, vermiculite, and pyrite in the presence of hydrogen sulfide (HS⁻) was studied under different environmental conditions. In systems containing biotite and vermiculite, the rate of CCl₄ transformation was dependent on the temperature, HS⁻ concentration, surface concentration, and Fe(II) content in the minerals. At 25°C, the half-life of CCl₄ with 1 mM HS⁻ was calculated to be 2600, 160, and 50 days for the homogeneous, vermiculite (114 m²/L) and biotite (55.8 m²/L) systems, respectively. The transformation rate with biotite and vermiculite was nearly independent of pH in the range 6 - 10 at constant HS⁻ concentration. The rate dependence on Fe(II) content of the sheet silicates suggested that the transformation occurs at surface sites where HS⁻ is associated with Fe(II).</p> <p>CCl₄ reacted relatively rapidly in 1.2-1.4 m²/L pyrite with >90% of the CCl₄ transformed within 12-36 days at 25°C. The observed rate law supports a heterogeneous reaction mechanism. The reactivity of CCl₄ with pyrite increased in the order: air-exposed pyrite/aerobic, air-exposed pyrite/HS⁻, air-exposed pyrite/anaerobic, and acid-treated pyrite/anaerobic but overall varied only by a factor of 2.5. The CCl₄ transformation products were observed to vary under different reaction conditions. Approximately 80-85% of the CCl₄ was transformed to CS₂ which hydrolyzed to CO₂. Only 5-15% of the CCl₄ was reduced to CHCl₃. In the pyrite systems, CO₂ was the major transformation product formed under aerobic conditions whereas CHCl₃ was largely formed under anaerobic conditions. Formation of some CS₂ was observed in all pyrite systems.</p>		
17. KEY WORDS AND DOCUMENT ANALYSIS		
a. DESCRIPTORS	b. IDENTIFIERS/OPEN ENDED TERMS	c. COSATI Field Group
ORGANICS ANAEROBIC AQUIFER KINETICS ABIOTIC TRANSFORMATION MINERAL CARBON TETRACHLORIDE	HYDROGEN SULFIDE BIOTITE VERMICULITE PYRITE PATHWAY	
18. DISTRIBUTION STATEMENT RELEASE TO THE PUBLIC	19. SECURITY CLASS (This Report) UNCLASSIFIED	21. NO. OF PAGES 62
	20. SECURITY CLASS (This page) UNCLASSIFIED	22. PRICE

DISCLAIMER

The information in this document has been funded wholly or in part by the United States Environmental Protection Agency under cooperative agreement CR-816776 to Stanford University. The report has been subjected to the Agency's peer and administrative review, and has been approved for publication as an EPA document. Mention of trade names or commercial products does not constitute endorsement or recommendation for use.

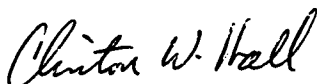
All research projects making conclusions or recommendations based on environmentally related measurements and funded by the Environmental Protection Agency are required to participate in the Agency Quality Assurance Project Plan. The procedures specified in this plan were used without exception. Information on the plan and documentation of the quality assurance activities and results are available from the Principal Investigator.

FOREWORD

EPA is charged by Congress to protect the Nation's land, air, and water systems. Under a mandate of national environmental laws focused on air and water quality, solid waste management and the control of toxic substances, pesticides, noise and radiation, the Agency strives to formulate and implement actions which lead to a compatible balance between human activities and the ability of natural systems to support and nurture life.

The Robert S. Kerr Environmental Research Laboratory is the Agency's center of expertise for investigation of the soil and subsurface environment. Personnel at the Laboratory are responsible for management of research programs to: (a) determine the fate, transport, and transformation rates of pollutants in the soil, the unsaturated and the saturated zones of the subsurface environment; (b) define the processes to be used in characterizing the soil and subsurface environment as a receptor of pollutants; (c) develop techniques for predicting the effect of pollutants on ground water, soil and indigenous organisms; and (d) define and demonstrate the applicability and limitations of using natural processes, indigenous to the soil and subsurface environment, for the protection of this resource.

Chlorinated solvents are among the most pervasive of ground-water contaminants and represent a significant fraction of total contamination incidents. This research was conducted to define rates of abiotic (chemical) transformation and fate mechanisms for carbon tetrachloride in the presence of natural mineral surfaces in aquifer systems. The data show that natural mineral surfaces can enhance the rate of degradation of carbon tetrachloride several orders of magnitude beyond that observed in homogeneous systems. This research demonstrates the importance of abiotic reactions in reducing concentrations of chlorinated solvents, especially in the presence of mineral surfaces typically found in aquifers. These types of reactions need to be considered and addressed in the use of models for predicting transport and fate of haloaliphatic compounds in the subsurface.



Clinton W. Hall

Director

Robert S. Kerr Environmental
Research Laboratory

ABSTRACT

This report addresses the ability of natural mineral surfaces to abiotically transform halogenated organic compounds in subsurface environments. The research focuses on carbon tetrachloride as the halogenated organic and biotite, vermiculite, and pyrite as the mineral surfaces. The CCl_4 transformation rates and products were quantified under different environmental conditions.

The disappearance of CCl_4 was significantly faster in the presence of mineral surfaces than in homogeneous solution. In systems containing the sheet silicates and HS^- , the rate of reaction was dependent on the temperature, HS^- concentration, surface concentration, and Fe(II) content in the minerals. At 25 °C, the half-life of CCl_4 with 1 mM HS^- was calculated to be 2600, 160, and 50 days for the homogeneous, vermiculite (114 m^2/L) and biotite (55.8 m^2/L) systems, respectively. The transformation rate with biotite and vermiculite was independent of pH over the range of 6 to 10 at constant $[\text{HS}^-]$. The heterogeneous transformation of CCl_4 with HS^- and biotite was first order with respect to the biotite surface concentration up to 280 m^2/L . Above 0.5 mM HS^- and 55.8 m^2/L biotite, the CCl_4 transformation rate was independent of $[\text{HS}^-]$ suggesting that the reaction is heterogeneous. In addition, the reactivity of CCl_4 with Aerosil 200 (amorphous silica)/ HS^- and the rate dependence on Fe(II) content of the sheet silicates suggest that the transformation occurs at sites where HS^- is associated with Fe(II) .

CCl_4 was observed to be relatively reactive with 1.2-1.4 m^2/L pyrite under all reaction conditions studied with >90% of the CCl_4 transformed within 12-36 days at 25 °C. A zeroth-order rate dependence on the CCl_4 concentration in the presence of 1.2 m^2/L pyrite supports a heterogeneous reaction mechanism. The reactivity of CCl_4 with pyrite increased in the order: air-exposed pyrite/aerobic, air-exposed pyrite/ HS^- , air-exposed pyrite/anaerobic, and acid-treated pyrite/anaerobic. The transformation rates only varied by a factor of 2.5 for all the conditions studied. An iron oxide coating, identified to be FeOOH using x-ray photoelectron spectroscopy, was detected on the pyrite that had been reacted aerobically. It was likely that this coating is responsible for the slower transformation rates observed under aerobic conditions.

The CCl_4 transformation products were observed to vary under different reaction conditions. In the sheet silicate/ HS^- systems, a new pathway to form CO_2 was identified. Approximately 80-85% of the CCl_4 was transformed to CS_2 which hydrolyzed to CO_2 . Only 5-15% of the CCl_4 was reduced to CHCl_3 . In the pyrite systems, CO_2 was the major transformation product formed under aerobic conditions whereas CHCl_3 was largely formed under anaerobic conditions. Formation of some CS_2 was observed in all pyrite systems, suggesting that CCl_4 or a reaction intermediate must react directly with pyrite-S.

This report was submitted in fulfillment of the grant EPA CR-816776 by the researchers in the Environmental Engineering and Science program, Department of Civil Engineering, Stanford University, under the sponsorship of the U.S. Environmental Protection Agency. This report covers the period September 7, 1990 to September 6, 1993, and work was completed as of September 6.

CONTENTS

SECTION 1	1
Research Objectives and Hypotheses	1
SECTION 2	3
SECTION 3	5
SECTION 4	6
Research Approach	6
Reference Solids, Pretreatments, and Reagents	6
Filling and Sealing of Ampules	7
Experiments with Sheet Silicates	7
Synthetic Solids Experiments	7
Experiments with Pyrite	8
Chemical Analyses	8
CCl ₄ and CHCl ₃ Analysis	8
CS ₂ Analysis	9
CO Analysis	9
Formate Analysis	9
Radiolabeled Products Analysis	9
Adsorbed Formate and CO ₂	10
Aqueous Pyrite Oxidation Products	10
Surface Pyrite Oxidation Products	10
Mineral Characterization	11
Sheet Silicate Characterization	11
Synthetic Solids Characterization	13
Pyrite Characterization	14
Kinetic Evaluation of Data	14
Adsorption	15
SECTION 5	
Transformation of CCl ₄ by Sheet Silicates	16
Effect of Biotite and Vermiculite on CCl ₄ Transformation	16

CCl ₄ Transformation Products.....	17
Temperature Dependence	22
pH Dependence	23
Effect of Solids Concentration	24
Effect of Sulfide Concentration	25
Effect of Ferrous Iron Content	26
Summary of Sheet Silicate Results	27
Transformation of CCl ₄ by Synthetic Solids	28
Transformation of CCl ₄ by Pyrite	29
Effect of Pyrite Pretreatment on CCl ₄ Transformation Rate	31
CCl ₄ Transformation Products.....	34
Pyrite Oxidation Products	39
Proposed Mechanism at Pyrite Surface	43
Summary of Pyrite Experiments	45
REFERENCES.....	46

LIST OF FIGURES

Figure 1:	XPS spectra of the Fe 2p peak for biotite reacted for 6 months in anaerobic Milli-Q water and 0.1 M HS ⁻ . No differences are observed in the oxidation state of iron in the two samples. Peaks are charge shifted by approximately 7.0 eV.....	12
Figure 2:	SEM micrograph of biotite cleavage sheet after reaction in anaerobic Milli-Q water for 6 months at 25 °C.....	13
Figure 3:	SEM micrograph of biotite cleavage sheet after reaction in 0.1 M HS ⁻ for 6 months at 25 °C.....	13
Figure 4:	First-order plots of CCl ₄ transformation with biotite (SC _{biotite} =55.8 m ² /L) and vermiculite (SC _{vermic} =114 m ² /L), [HS ⁻]=1 mM, pH=8.6 at 50 °C.....	17
Figure 5:	CCl ₄ transformation products from reaction with [HS ⁻]=1mM, SC _{biotite} =55.8 m ² /L, pH=8.8 at 50 °C. Lines represent best fit using eqs. 8, 12, and 13.....	18
Figure 6:	Carbon disulfide (CS ₂) was identified as an intermediate of CCl ₄ transformation by the agreement between the CS ₂ fraction measured by gas chromatography and the “unidentified” volatile fraction measured from ¹⁴ C experiments.	19
Figure 7:	Proposed CCl ₄ transformation pathways in HS ⁻ solution containing biotite. Shadowed boxes are products and intermediates detected in this study. Compounds in brackets are intermediates proposed from the literature (as cited in Criddle and McCarty, 1991) and this report. Reaction pathways with dashed arrows have been observed in other studies (as cited in Criddle and McCarty, 1991).....	20
Figure 8:	CCl ₄ transformation rate at 1 mM HS ⁻ , 50 °C, and 55.8 m ² /L biotite or 114 m ² /L vermiculite in the pH range of 6-10. Error bars are 95% confidence intervals around k' _{homo} or k' _{hetero}	24
Figure 9:	The effect of biotite surface concentration (SC _{biotite}) on the CCl ₄ transformation rate (k' _{hetero}) at 50 °C. The best-fit line for the data at 11.2 and 55.8 m ² /L passes through the origin. Error bars are 95% confidence intervals.....	25
Figure 10:	The effect of HS ⁻ concentration on the CCl ₄ transformation rate (k' _{hetero}) and the fit to the proposed rate law (eq. 3) with SC _{biotite} =55.8 m ² /L at 50 °C. Above [HS ⁻] = 0.5 mM, the rate shows a zeroth-order dependence on [HS ⁻] (b ₂ =0). When [HS ⁻] < 0.5 mM, b ₂ is estimated to be 1.34 or 1.16±0.21 using k' _{hetero} and k' _{i,hetero} data, respectively. Error bars are 95% confidence intervals.....	26
Figure 11:	The effect of bulk ferrous iron content in the minerals, muscovite, vermiculite, and biotite on k' _{hetero} at 50 °C.	27

Figure 12:	Zeroth-order dependence of the disappearance of CCl_4 in the presence of air-exposed pyrite reacted under aerobic and anaerobic conditions at 25 °C. The control represents the disappearance of CCl_4 in a 1 mM NaCl anaerobic solution.....	32
Figure 13:	The disappearance of 100 mM CCl_4 with 1.2 m ² /L pyrite reacted anaerobically at 25 °C. Appearance of formic acid was measured with an ion chromatograph.	35
Figure 14:	Disappearance of CCl_4 in the presence of pyrite under aerobic conditions at 25 °C. Appearance of the products, CS_2 and CO_2 , with model results assuming the only path to form CO_2 is $\text{CCl}_4 \rightarrow \text{CS}_2 \rightarrow \text{CO}_2$	37
Figure 15:	Disappearance of CCl_4 in the presence of pyrite under aerobic conditions at 25 °C. Appearance of the products, CS_2 and CO_2 , with model results assuming the only path to form CO_2 from CCl_4 is: $\text{CCl}_4 \rightarrow \text{Intermed.} \rightarrow \text{CS}_2 \rightarrow \text{CO}_2$	38
Figure 16:	Disappearance of CCl_4 in the presence of acid-treated pyrite under anaerobic conditions at 25 °C. Appearance of the products, CS_2 and CO_2 , with model results assuming the only path to form CO_2 is: $\text{CCl}_4 \rightarrow \text{CS}_2 \rightarrow \text{CO}_2$	39
Figure 17:	XPS spectra comparing S 2p peak for pyrite reacted under anaerobic conditions in the presence and absence of 1 mM CCl_4	40
Figure 18:	XPS spectra of Fe 2p peak of air-exposed pyrite reacted aerobically. The Fe(III) peaks are indicative of an iron oxide coating on the pyrite.....	40
Figure 19:	XPS spectra of O 1s peak of air-exposed pyrite reacted aerobically. The peaks at 530.1 and 531.2 eV coincide with the O 1s peak for FeOOH (Moulder et al., 1992).....	41
Figure 20:	XPS spectra of the S 2p peak comparing fresh-ground pyrite reacted anaerobically with air-exposed pyrite reacted aerobically. There is no significant difference in the S 2p peak shapes and binding energies under these reaction conditions.	42
Figure 21:	Proposed CCl_4 transformation pathways with pyrite. Compounds in shadowed boxes are measured intermediates or products. Compounds in brackets are proposed intermediates.	44

LIST OF TABLES

Table 1:	Specific surface area determined by BET and iron content for minerals and synthetic solids.	11
Table 2:	Pseudo-first-order rate constants obtained for CCl ₄ transformation pathways using eqs. 8, 12, and 13.	23
Table 3:	Arrhenius parameters for CCl ₄ transformation with 1 mM HS ⁻ at 50°C. Ea and lnA were calculated using k _{i,het} for biotite and vermiculite and k _i was used for the homogeneous systems.	23
Table 4:	Results of CCl ₄ transformation in systems containing HS ⁻ , gibbsite and Aerosil 200 at 50°C.	29
Table 5:	Zeroth-order rate constants for CCl ₄ transformation with pyrite reacted under aerobic and anaerobic conditions at 25 °C.	32
Table 6:	Comparison of pyrite oxidation rate by CCl ₄ with literature rates of oxidation by O ₂ , Fe ³⁺ , and H ₂ O ₂ at room temperature.	33
Table 7:	CCl ₄ product distribution from reaction with pyrite under aerobic and anaerobic conditions at 25 °C.	34
Table 8:	Rate constants for the disappearance of CCl ₄ and appearance of intermediates and products from reaction with pyrite under aerobic and anaerobic conditions at 25 °C.	36
Table 9:	Effect of environmental conditions on S:Fe(II) in the near-surface of pyrite where S:Fe(II) was determined using XPS.	43

ACKNOWLEDGMENTS

We thank Art F. White for suggesting that we study oxygenated systems in the pyrite studies, David King for helping us solve differential equations and Stephen R. Hutchins for serving as our Project Officer.

SECTION 1

INTRODUCTION

Halogenated organic compounds are prevalent contaminants in ground water and are often components of landfill leachate and hazardous waste. Recent reports suggest a link between chlorinated hydrocarbons and increased incidence of many illnesses ranging from breast cancer to endocrine disorders (Hileman, 1993). Although there are proposals to ultimately eliminate use of many of these anthropogenic compounds in our society, their current widespread use predicates the need to understand the fate of these compounds in subsurface environments. Until recently, most studies of organic contaminants were conducted at the "system" level in which the disappearance of these compounds in sediment slurries was investigated without an attempt to understand the processes controlling the disappearance. In 1986, Macalady et al. promulgated the need to understand the chemical, physical, and biological processes that potentially control the fate of these compounds, ultimately leading to a predictive capability.

An example of a progression from the "system" level to the process level is the transformation of hexachloroethane (HCA) by sediment samples from the Canadian Forces Base in Borden, Ontario. Criddle et al. (1986) found that HCA is transformed to tetrachloroethylene (PCE) in sterilized Borden sediment slurries. Subsequently Curtis (1991) identified the reactive component of the Borden sand to be organic matter associated with the sediment fraction containing quartz, feldspars, and carbonate minerals. Curtis (1991; Curtis and Reinhard, 1993) further investigated the reactivity of humic substances and model compounds with HCA and other haloaliphatic organics at the process level. Although this work does not allow prediction of the fate of HCA under diverse environmental conditions, it did provide a deeper understanding of the processes that may be controlling reactivity in some sediment systems.

In his studies to identify the reactive component in Borden sand, Curtis (1991) suggested that ferrous iron bearing minerals may play a role in the transformation of haloaliphatic compounds. Although they were not the major reductant in the case of Borden sand, ferrous iron bearing minerals can play a major role in other environments. Anderson et al. (1992; 1994) proposed that such minerals were responsible for the reduction of Cr(VI) to Cr(III) in a sand and gravel aquifer at Otis Air Force Base, Cape Cod, MA. Furthermore, at the same site, Barber et al. (1992) found that chlorinated benzenes were adsorbed to organic matter associated with the iron bearing minerals. If the haloaliphatics are associated with organic matter at iron bearing phases, ferrous iron bearing minerals may be able to reduce haloaliphatic compounds at environmentally significant rates.

Research Objectives and Hypotheses

The objectives of this research were to test the ability of ferrous iron bearing minerals to abiotically transform haloaliphatic compounds in sulfidic environments and to identify the organic's transformation products. The work focused largely on carbon tetrachloride as the halogenated organic and biotite, vermiculite, and pyrite as the ferrous-iron bearing minerals. CCl₄ was chosen as the compound of interest because it is a contaminant frequently found in ground water, it is a suspected human carcinogen (Sax and Lewis, 1987), it causes ozone depletion, and it is a greenhouse gas (Rowland, 1991). Additionally, CCl₄ is known to react relatively rapidly in the presence of reductants (for example, Castro and Kray, 1963; 1966). Biotite and vermiculite are sheet silicates that are commonly found as detrital materials in

sedimentary rocks (Deer et al., 1982) and sulfidogenic conditions are often observed in plumes of hazardous waste and landfill leachate (Barbash and Reinhard, 1989a). To obtain additional insight into the reaction mechanism of CCl_4 with the sheet silicates and sulfide, experiments were conducted with muscovite, pyrite, and the synthetic solids, Aerosil 200 (amorphous silica) and gibbsite. In-depth studies of pyrite reactivity were conducted because pyrite, an iron sulfide mineral, is ubiquitous in sulfidic environments (Howarth and Teal, 1979; Luther et al., 1982; Lord and Church, 1983) and is potentially the most significant environmental player of the systems studied.

It was hypothesized that:

- (1) CCl_4 is transformed faster in the presence of mineral surfaces than in homogeneous solution;
- (2) the rate of transformation is a function of the reaction conditions such as the type of mineral, iron content, pH, temperature, sulfide concentration, presence of oxygen, and solids concentration;
- (3) the CCl_4 transformation products will vary under different reaction conditions.

The research approach used to address these hypotheses and an overview of the research project are delineated below. Additional hypotheses such as the influence of natural organic matter, competing oxidants, and co-solvents on the CCl_4 transformation rates and products in heterogeneous systems were not addressed in this project.

SECTION 2

SUMMARY AND CONCLUSIONS

This research demonstrates, for the first time, that mineral surfaces may play a significant role in the fate and transport of haloaliphatic compounds in subsurface environments. The results of this work provide insight into the rates of CCl_4 transformation under different environmental conditions, the CCl_4 transformation products, and the mechanism of CCl_4 transformation at mineral surfaces. The specific conclusions that can be drawn from this work are as follows:

(1) *The disappearance of CCl_4 in sulfidic systems was significantly faster in the presence of mineral surfaces (biotite, vermiculite, pyrite, and Aerosil 200) than in homogeneous solution.* In sulfide solutions containing biotite, vermiculite, or Aerosil 200, CCl_4 was transformed an order of magnitude faster than in homogeneous systems containing only HS^- . At 25 °C, the half-life for the disappearance of CCl_4 in the presence of 1 mM HS^- was 2600, 160 and 50 days for the homogeneous, vermiculite (114 m^2/L), and biotite (55.8 m^2/L) systems, respectively. In addition, the reaction of CCl_4 with pyrite at 25°C was orders of magnitude faster than reactions with 1 mM HS^- or 0.1 mM Fe(II) in solution at 50°C. In the pyrite systems 50% of the CCl_4 reacted within 6-20 days at 25 °C. These results along with additional evidence suggest that the reaction with CCl_4 is heterogeneous.

(2) The disappearance of CCl_4 in the sheet silicate and Aerosil 200 systems followed first order kinetics with respect to the CCl_4 concentration. In the presence of pyrite, however, the disappearance followed zeroth-order kinetics (MDL to 1 μM) with respect to the CCl_4 concentration, indicating that reactive surface sites were saturated with CCl_4 , and that the rate of reaction was not dependent on the solution concentration. The possible reaction mechanisms of CCl_4 degradation at the Aerosil 200 interface by HS^- remain to be investigated.

(3) *The rate of transformation of CCl_4 with the sheet silicates and sulfide depended on the following reaction conditions: temperature, surface concentration, sulfide concentration, and ferrous iron content in the minerals.* The CCl_4 transformation rate was investigated over the range of 6-10 at constant $[\text{HS}^-]$ showed and showed a very shallow minimum at near-neutral pH. The role of the proton and the hydroxide ion in the rate-limiting step could not be elucidated. The Arrhenius parameters were calculated from the temperature dependence studies. The activation energies were 122, 91, and 60 kJ/mol for the homogeneous, vermiculite and biotite systems, respectively. The disappearance of CCl_4 was first order with respect to the surface concentration up to a surface concentration of 280 m^2/L biotite. The dependence on sulfide concentration was studied over a range of 0.02-4 mM HS^- at a fixed surface concentration. Below 0.5 mM HS^- , the CCl_4 transformation rate was roughly first order with respect to $[\text{HS}^-]$, whereas above 0.5 mM HS^- , the transformation rate was independent of $[\text{HS}^-]$. These results suggest that the biotite surface sites are saturated with HS^- above 0.5 mM $[\text{HS}^-]$. Lastly, a relationship between the ferrous iron content in muscovite, vermiculite, and biotite, and the CCl_4 transformation rate intimate that ferrous iron plays a role in the reaction with CCl_4 .

(4) *The rate of transformation of CCl_4 with pyrite varied with reaction conditions in the following order: air-exposed pyrite/aerobic \leq air-exposed pyrite/sulfide $<$ air-exposed pyrite/anaerobic \leq acid-treated pyrite/anaerobic.* The rate constants varied by only a factor of

2.5 for all the conditions studied. HS^- inhibited the CCl_4 transformation rate by pyrite relative to systems reacted anaerobically in the absence of HS^- . The fresh-ground/anaerobic data could not be included in this evaluation because of the large scatter in the data, probably caused by heterogeneity introduced by grinding.

(5) *The CCl_4 transformation products varied greatly as a function of the reaction conditions.* In the sheet silicate/sulfide systems CS_2 was identified as a major intermediate that hydrolyzed to CO_2 , accounting for >85% of the CCl_4 transformed. The hydrolysis of CS_2 establishes a new pathway to form CO_2 anaerobically. In the pyrite systems, CS_2 was detected under all reaction conditions, suggesting that CCl_4 or an intermediate must react directly with the pyrite surface. Under aerobic conditions, CO_2 was the major transformation product (80%), but kinetic modeling could not resolve the pathway to form CO_2 . At this point it is not known if CO_2 is formed via reaction of the trichloromethyl radical with O_2 , or the CS_2 hydrolysis pathway. In the fresh-ground pyrite systems, roughly 50% of the CCl_4 was transformed to CHCl_3 . In all systems studied, formate and carbon monoxide were minor products.

(6) Under aerobic conditions, an iron oxide coating developed on the pyrite surface. Using x-ray photoelectron spectroscopy (XPS), this coating was identified to be FeOOH . It is likely that this coating is responsible for the slower reaction rates and different product distribution measured under aerobic conditions.

(7) Reaction of CCl_4 with the model solids, Aerosil 200 and gibbsite, provided insight into the transformation mechanism of CCl_4 by the sheet silicates in the presence of sulfide. In systems containing HS^- , CCl_4 was reactive with Aerosil 200 and not with gibbsite ($\gamma\text{-Al}(\text{OH})_3$), demonstrating that HS^- may be associated with silica in the sheet silicate experiments. However, the reactivity with Aerosil was not as great as the sheet silicates, suggesting that ferrous iron was playing a role in the transformation of CCl_4 .

(8) *The rate of transformation of CCl_4 with the sheet silicates was dependent on both the ferrous iron content and the sulfur concentration, indicating that the reaction occurs at sites where sulfide is associated with structural ferrous iron.* It is unlikely that CCl_4 is reacting with secondary iron sulfide phases because (a) the CCl_4 product distribution formed in the fresh-ground pyrite system was very different from that formed in the sheet silicate system; and (b) the CCl_4 transformation rate was independent of sulfide concentration above a certain level. If secondary iron sulfides are controlling the CCl_4 transformation rate, higher sulfide concentrations should precipitate more iron sulfides through enhanced weathering, thereby causing an increase in the CCl_4 transformation rate.

(9) In the pyrite system, the near-surface was depleted of iron after reaction in water, while the oxidation state of the pyrite-S appeared to remain the same. *The high sulfur concentration at the near-surface makes it likely that pyrite-S is the reductant of CCl_4 , rather than pyrite-Fe.* At circumneutral pH, these surface sulfur sites are negatively charged. Under anaerobic conditions it is proposed that an electron is transferred from FeSS^- to CCl_4 and that the intermediate FeSSCCl_3 is formed. Both the surface and solution conditions dictate the decomposition pathway of this intermediate. Under aerobic conditions the site of electron transfer is not determined as it may occur across the FeOOH coating or at unoxidized sulfur sites.

SECTION 3

RECOMMENDATIONS

The results of this study show that mineral surfaces may play a significant role in the fate of halogenated organics in the environment. Although they can be quantitatively applied to natural systems only with some difficulty, these data show that rate constants measured in deionized water will greatly underpredict the actual transformation rates. In pyrite- or sulfide-rich environments, abiotic transformation pathways may be significant on the timescale of ground water transport. Predictive capabilities are complicated at this point due to the confounding effects of natural organic matter, co-solvents, competing oxidants, and microbial activity. To address these issues, continued research to further understand the surface chemistry of pyrite, the CCl_4 transformation pathway at the pyrite surface, and the reactivity of CCl_4 and other polyhalogenated aliphatics under field conditions is necessary. This work will ultimately lead to predictive capabilities.

The pyrite surface was relatively reactive with CCl_4 even under aerobic conditions; therefore, it is conceivable that a pyrite-based treatment system could be engineered. Further studies would have to be conducted in order to (1) identify the rate determining step of the reaction, (2) test the efficiency of the method in column and batch reactors, (3) control the CCl_4 product distribution, and (4) measure the pyrite oxidation products and ensure that they are harmless. In addition, the engineered system would have to be tested with other haloaliphatics to see if they could also be transformed and if they inhibited or effected the transformation of CCl_4 .

SECTION 4

MATERIALS AND METHODS

Research Approach

The primary goal of this research was to test the ability of mineral surfaces to transform CCl_4 under different environmental conditions. The base case reactions conditions to measure the disappearance rate of $1\ \mu\text{M}$ CCl_4 in the biotite, vermiculite, and synthetic solid systems were $\text{pH}=7.5\text{--}8.5$, $\text{temperature}=50\ ^\circ\text{C}$, and $[\text{HS}^-]=1\ \text{mM}$. The solids concentrations for the base case were $55.8\ \text{m}^2\ \text{biotite/L}$, $114\ \text{m}^2\ \text{vermiculite/L}$, $700\ \text{m}^2\ \text{Aerosil/L}$, and $100\ \text{m}^2\ \text{gibbsite/L}$. Controls were established by reacting CCl_4 with HS^- at the same temperature and pH , but in the absence of the solids. To study the effects of environmental conditions on the reaction rate, experiments with biotite were conducted over a pH range of 6–10, temperature range of $37.5\text{--}62.7\ ^\circ\text{C}$, solids concentration of $11.2\text{--}280\ \text{m}^2/\text{L}$, and $[\text{HS}^-]=0.02\text{--}4\ \text{mM}$.

For all pyrite/ CCl_4 transformation rate and product studies, $1\ \mu\text{M}$ CCl_4 was reacted in aqueous systems containing $1.2\text{--}1.4\ \text{m}^2/\text{L}$ pretreated pyrite at $\text{pH}\ 6.5$ and $25\ ^\circ\text{C}$, except the experiments conducted with sulfide which were at $\text{pH}\ 7.75$. Since a pH buffer was not used because of the potential confounding effects on CCl_4 reactivity, experiments were conducted in a $1\ \text{mM}$ NaCl ionic medium. Controls were established by reacting CCl_4 under the same conditions in the absence of pyrite in addition to reacting CCl_4 in homogeneous solutions of $\text{Fe}^{2+}_{\text{aq}}$ or HS^- .

For the studies of the pyrite oxidation products, $0.1\text{--}1\ \text{mM}$ CCl_4 was reacted with large particles of pretreated pyrite ($0.2\ \text{g}$) to maximize oxidation on a small pyrite surface area. Controls were established by reacting pyrite under the same conditions, but in the absence of CCl_4 . These experiments were designed to measure the oxidation due to both pyrite pretreatments and reaction with CCl_4 .

Reference Solids, Pretreatments, and Reagents

Biotite, vermiculite, and muscovite were obtained from Ward's Scientific Establishment, Inc. (Rochester, NY). The minerals were wet ground with an Osterizer blender (using deoxygenated Milli-Q water, Millipore Corp., Bedford, MA) in an anaerobic glove box (Coy Products, Ann Arbor, MI) which had a $90\%\ \text{N}_2/10\%\ \text{H}_2$ atmosphere. After grinding, the minerals were freeze-dried, dry-sieved, and stored in the anaerobic glove box. The $200\text{--}50$ mesh U.S. Standard ($75\text{--}300\ \mu\text{m}$) size fraction was used for the experiments. Aerosil 200 ($>99.8\%\ \text{SiO}_2$, Degussa, Ridgefield Park, NJ) and gibbsite (ALCOA, Alcoa Center, PA) were rinsed twice with Milli-Q water before using.

Pyrite (Zacatecas, Mexico) was obtained from Ward's Scientific Establishment, Inc. (Rochester, NY). All grinding and pretreatment of the pyrite was conducted in a glovebox containing a $90\%\ \text{N}_2/10\%\ \text{H}_2$ atmosphere (Coy Products, Ann Arbor, MI). Pyrite was ground with a ceramic mortar and pestle, sieved to $75\text{--}300\ \mu\text{m}$, sonicated in deoxygenated Milli-Q water, and "air-dried" in the glovebox. Acid-treatment was conducted in the glovebox using $20\ \text{g}$ batches of pyrite. Sonicated pyrite was washed twice for 2 minutes with $20\ \text{mL}$ of $1\ \text{N}$ HCl , rinsed 10 times with $40\text{--}\text{mL}$ aliquots of deoxygenated Milli-Q water, and "air-dried" in the glovebox. The sonicated pyrite to be exposed to air was placed in an amber-glass screw-top vial. The vial was removed from the glovebox and opened to the atmosphere for 3 days.

The following compounds were obtained from commercial sources and used as received: carbon tetrachloride (>99%), trichloroethylene (99%), and chloroform (99%). Radiolabeled (^{14}C) CCl_4 was obtained from Sigma Chemical Co. (St. Louis, MO), diluted in Milli-Q water and stored in flame-sealed glass ampules at 4 °C in the dark. Sodium sulfide ($\text{Na}_2\text{S}\cdot 9\text{H}_2\text{O}$, 98%) and carbon disulfide (>99%) were stored in an Ar-filled glove bag. Individual crystals of sodium sulfide were rinsed with deoxygenated Milli-Q water to remove oxidation products and wiped dry with cellulose tissue before use. Anhydrous sulfate (Na_2SO_4 , >99%) and sulfite (Na_2SO_3 , >99.5%) were stored in a desiccator. A 0.1 N thiosulfate standard solution (Fluka Chemical Co., Buchs, Switzerland) was stored in the anaerobic glovebox. Anhydrous pentane (>99%) was stored under a nitrogen atmosphere to prevent contamination by halogenated organics.

Filling and Sealing of Ampules

Experiments with Sheet Silicates

All transformation and adsorption studies were conducted in flame-sealed glass ampules because the reaction times were on the order of weeks to months at elevated temperature (50°C). The ampule method was based on and adapted from Barbash and Reinhard (1989b). Ampules were washed with 10% nitric acid, rinsed with deionized water and oven dried overnight at 110 °C. Ampules were weighed and filled with a known amount of sheet silicate. To minimize Fe(II) oxidation in the autoclave, mineral-filled ampules were autoclaved under a nitrogen atmosphere. The nitrogen atmosphere was achieved by placing the ampules in a pressure cooker that contained 100 mL of water. The pressure cooker was evacuated three times to 75 mm Hg, backfilled with 99.99% nitrogen, and autoclaved at 121 °C for 20 min (Curtis, 1991). After autoclaving, the ampules were placed in the anaerobic glove box to allow oxygen to exsolve for a minimum of 2 days. Stock solutions of sulfide were made fresh daily by transferring pre-weighed and washed sodium sulfide crystals into 50 mL of deoxygenated water in the glovebox. The amount of HCl or sulfide stock used to make the sulfide solution was determined by the parameters of a given experiment. This sulfide solution will herein be referred to as the "buffer". A pH buffer or background electrolyte was not used to eliminate potential confounding effects on the CCl_4 transformation rate.

Ampules were filled with approximately 13.5 mL of buffer that was filtered through a sterilized 0.2 μm nylon filter (Nalgene Corp., Rochester, NY). Each ampule was covered with a polyvinylidene chloride (SaranTM) sheet, secured at the neck with a 3/16" inner-diameter ring of latex tubing, removed from the glove box, spiked with an appropriated volume of an aqueous solution saturated with CCl_4 , and flame-sealed under a stream of nitrogen. After sealing, ampules were weighed to obtain the exact amount of buffer added, and placed in the dark in a constant temperature water bath (± 0.1 °C) for the duration of the experiment. Weight loss upon sealing was less than 0.005% and was not considered significant. Daily to weekly, ampules were removed from the bath, shaken by hand, and returned to the bath. At each sampling time, two ampules for each experimental condition were removed from the constant-temperature bath and preserved at 4 °C in the dark until they could be extracted. Before extraction, ampules were centrifuged at 4 °C and 1400 g for 20 min.

Synthetic Solids Experiments

Transformation studies in the presence of Aerosil 200 and gibbsite were also conducted in 10-mL flame-sealed glass ampules. However, due to the small particle size, the solids were added to the ampules as a slurry. The slurry was made outside the glove box and autoclaved for 20 minutes at 120°C. The slurry was deoxygenated by bubbling the solution with nitrogen which

passed through a sterile 0.2 μm nylon filter for 1 hour. The deoxygenated slurry was placed in the glove box and bubbled with the glove box atmosphere for 30 minutes. Sodium sulfide was added to the slurry at this time. To fill the ampules, a sterilized syringe with a sterilized spinal needle was fitted to the slurry with sterilized PTFE tubing and three-way valve. Once the ampules were filled, they were covered with a SaranTM sheet and secured at the neck with a 3/16-in. inner-diameter ring of latex tubing. All other procedures in the synthetic solids experiments were identical to those described above, except the ampules were centrifuged at 2800 g for 30 min.

Experiments with Pyrite

Transformation studies in the presence of pyrite were conducted in 10-mL flame-sealed glass ampules that were acid washed, oven dried, and placed in the anaerobic glovebox to outgas for 2 days (Kriegman-King and Reinhard, 1992). Air-exposed pyrite was placed back into the glovebox. For all reaction conditions, 0.2 g (± 0.003 g) pyrite was weighed into the ampules.

For all conditions, except the aerobic system, a 1 mM NaCl solution was deoxygenated with N_2 for 1 hour and placed in the glovebox. The NaCl solution was then sparged with glovebox air for a minimum of 30 min. Sulfide solutions were made as described above. Ampules were filled with approximately 13.5 mL of either the NaCl or sulfide solution that was filtered through a sterile 0.2 μm nylon filter (Nalgene Corp., Rochester, NY). Once the ampules were filled, they were spiked and sealed while taking precautions to maintain anaerobic conditions (Barbash and Reinhard, 1989b; Kriegman-King and Reinhard, 1992). The XPS and pyrite-sulfur oxidation-experiments were conducted at 0.1-1 mM CCl_4 . CCl_4 was added as a methanolic spike rather than an aqueous spike. Sealed ampules were weighed and placed in the dark in a 24.7 $^\circ\text{C}$ constant-temperature water bath (± 0.1 $^\circ\text{C}$) for the duration of the experiment.

For ampules to be reacted aerobically, the 1 mM NaCl solution was sparged with laboratory air for 45 min to strip any residual CHCl_3 from the Milli-Q water. Pyrite-filled ampules were removed from the glovebox and filled with approximately 13.5 mL of a 1 mM NaCl solution that was also filtered. Ampules were spiked with CCl_4 and immediately flame-sealed.

For all conditions, ampules were shaken manually once daily for the first 10 days of reaction and then every other day until the experiment was complete. At each sampling time, two ampules for each experimental condition were removed from the constant-temperature water bath, centrifuged at 4 $^\circ\text{C}$ and 2800 g for 20 min, and stored at 4 $^\circ\text{C}$ for a maximum of 3 hours until preparation for analysis.

Chemical Analyses

CCl_4 and CHCl_3 Analysis.

Reaction solutions were extracted in 2.9-mL glass vials with PTFE/silicone septum-lined screw top caps. Ampules were cracked open, 2 mL of aqueous solution were transferred to an extraction vial containing 0.5 mL of pentane, and the vial was shaken for 15 sec. Extraction vials were stored inverted at -5 $^\circ\text{C}$ in the dark for up to 24 h before GC analysis. Extraction vials were removed from the freezer, defrosted to room temperature, and spiked with an appropriate amount of internal standard (trichloroethylene). Vials were mixed on a shaker table for 30 min at 350 rpm. The extractant was analyzed for CCl_4 and CHCl_3 using a Hewlett-Packard 5890 gas chromatograph equipped with a ^{63}Ni electron capture detector and a DB-1 column (J&W Scientific, Rancho Cordova, CA), 15 m x 0.535 mm, with a film thickness of 1.5 μm . Helium

was used as the carrier gas and Ar/CH₄ as the make-up gas. The gas chromatograph was calibrated daily with a minimum of 5 calibration standards and duplicate measurements were made for each sample or standard. If the measurements did not agree within 10%, a third injection was made.

CS₂ Analysis

A 2.9-mL aliquot of reaction solution from the ampules was transferred to an extraction vial (described above) to fill the vial with no headspace. The vials were stored at 4 °C in the dark for up to 48 h before GC analysis. Aqueous samples (2-2.4 mL) were analyzed for CS₂ using a Tekmar Model ALS Purge and Trap with a Hewlett-Packard 5890 gas chromatograph equipped with a 10.0 eV Tracor photoionization detector and a Quadrex 007-502 column (Quadrex Corp., New Haven, CT), 75 m x 0.535 mm, with a film thickness of 2.5 µm. Helium was both the carrier gas and the make-up gas. The GC was calibrated daily using external standards at a minimum of four calibration levels.

CO Analysis

CO was determined by transferring a 7.1 mL aliquot of aqueous solution from an ampule to an 8.7 mL vial with a PTFE/silicone septum-lined screw top cap. The vial was shaken at 350 rpm for 10 min to equilibrate the CO partitioning between the headspace and the aqueous phase. A 0.4 mL headspace sample was analyzed on a Reduction Gas Detector (Trace Analytical, Menlo Park, CA) using 30 mL/min air as the carrier gas. The gas phase CO concentration was calculated by comparing the peak height to CO gas standards (Scott Specialty Gases, San Bernadino, CA). The total amount of CO was calculated using a Henry's constant of 0.96 atm·m³/mol at 20 °C (Tchobanoglous and Schroeder, 1985).

Formate Analysis

An ion chromatograph (Dionex Series 4000i) equipped with a conductivity detector was used to measure the formate concentration from reaction of CCl₄ with pyrite. A Dionex AS-4A separator column was used with 5 mM borate eluent at a flow rate of 2.0 mL/min. The detection limit for formate was approximately 1 µM. Although the aqueous non-volatile fraction was identified to be formate by matching retention times of an unknown peak formed in pyrite systems with formate standards on the ion chromatograph, formate was not directly quantified in most of these systems. Herein, the non-volatile fraction is assumed to be formate.

Radiolabeled Products Analysis

To determine the product distribution in experiments with radiolabeled substrate, three 1-mL aliquots of reaction solution were taken from each ampule. Aliquot 1 was acidified with 0.2 mL of 1 N H₂SO₄ and purged with N₂ for 10-15 min. This procedure stripped the volatiles and CO₂ from solution, leaving the non-volatiles behind. After purging, 10 mL of Universol (ICN Biomedicals, Inc., Irvine, CA) liquid scintillation cocktail were added to the sample. Aliquot 2 was treated with 0.2 mL of 1 N NaOH and purged for 10-15 min, thereby stripping only the non-CO₂ volatiles. Again, 10 mL of scintillation cocktail were added to the sample after purging. Aliquot 3 was immediately added to 10 mL of scintillation cocktail containing 0.2 mL 1 N NaOH (not purged) to determine the total radioactivity. The CO₂ fraction was then calculated by subtracting the counts in aliquot 1 from those in aliquot 2; and the volatile fraction was calculated as the difference between the counts in aliquot 3 and those in aliquot 2. The efficiency of this method to strip CO₂ under acidic conditions and to retain CO₂ under basic conditions was tested by adding 0.13-0.56 mL of 1 N H₂SO₄ or 1 N NaOH, respectively, to the 1 mL aliquots. There was no significant difference in the results with increasing amounts of acid or base added.

All samples were then counted twice on a Packard Tricarb Model 4530 liquid scintillation counter for 10 min. Measured counts-per-minute were converted to disintegrations-per-minute using the external standard method.

Adsorbed Formate and CO₂

Adsorbed formate and CO₂ were obtained using a presumptive method. The supernatant was removed from the ampules using a syringe, 0.4 mL of 1 M H₂SO₄ or 1 M NaOH was added to the ampules, and ampules were allowed to sit for 10 min. One-mL dilution water was added to the ampules and mixed with the slurry. After letting the pyrite settle for 10 min, a 1-mL aliquot of the aqueous phase was placed into a scintillation vial, purged with N₂ for 15 min, and counted on a Packard Tricarb Model 4530 liquid scintillation counter. The extreme acidic and basic conditions presumably desorbed both the CO₂ and formate. The pH_{pzc} of pyrite has been reported to be 1.2 (Fornasiero et al., 1992). By purging the system with N₂, the CO₂ was stripped from solution at acid pH leaving the "adsorbed" formate in solution, whereas the basic solution retained both the "adsorbed" CO₂ and formate. The loss of "adsorbed" CO₂ via precipitation of carbonate minerals at high pH was assumed insignificant because the supernatant containing metal ions, such as Fe²⁺, was removed. This method did not allow measurement of the adsorbed volatile fraction.

Aqueous Pyrite Oxidation Products

For analysis of potential aqueous pyrite oxidation products SO₃²⁻, SO₄²⁻, S₂O₃²⁻, centrifuged ampules were cracked open in the anaerobic glovebox to prevent oxidation of SO₃²⁻ and S₂O₃²⁻. A 0.5-mL aliquot of supernatant was placed in a 10-mL volumetric flask and diluted to 10 mL with deoxygenated Milli-Q water. A portion of diluted sample was then transferred to a 2.9-mL glass vial to fill the vial with no headspace and sealed with a PTFE/silicone septa-lined cap. The sample vials were stored in the glovebox up to 6 hours and were removed from the glovebox immediately before analysis. Standards at three calibration levels were made in the glovebox with deoxygenated Milli-Q water and treated identically to the unknowns. Samples were withdrawn from the vials with a 2-mL gas-tight syringe that had been filled with N₂ and analyzed on a Dionex Series 4000i ion chromatograph equipped with a conductivity detector. A Dionex AS-5 separator column with 4.5 mM Na₂CO₃/2.0 mM NaOH eluent at 1.5 mL/min was used to separate SO₃²⁻, SO₄²⁻, and S₂O₃²⁻.

Surface Pyrite Oxidation Products

Ampules were cracked open in the glovebox, and the supernatant was removed. Using tweezers and a microbiological loop, a large particle of pyrite was removed from the ampule, dipped in deoxygenated Milli-Q water, and adhered to an XPS sample holder using double-stick tape or silver paint. Samples were allowed to dry overnight in a desiccator in the glovebox. Within the glovebox, the desiccator was transferred to a glovebag and sealed with low-oxygen permeable tape (Coy Products, Ann Arbor, MI). The sample holder was transferred into the XPS instrument by sealing the glovebag opening around the transfer chamber of the instrument and flushing the glovebag with nitrogen. The desiccator was opened and the sample holder was placed in the transfer chamber. XPS analysis was conducted using a Surface Science S-Probe equipped with a monochromatic Al-K α x-ray source. A spot-size of 150 x 800 μ m was used with a pass energy of 150 eV for broad scans and 50 eV for narrow scans. Normalized concentrations were calculated for the peak of interest by dividing the peak area by a sensitivity factor comprising the Scofield cross-section (Scofield, 1976) and the relative kinetic energy of the photoelectrons (Hyland and Bancroft, 1990).

Mineral Characterization

Sheet Silicate Characterization

Specific surface area and iron content of the sheet silicates are shown in Table 1. Surface area was measured on an Acusorb 2100E surface area analyzer by the BET method using krypton adsorption. Ferrous iron and total iron in the sheet silicates were measured using a modification of several 1,10-phenanthroline methods (Fadrus and Maly, 1975; Begheijn, 1979; Fritz and Popp, 1985). A 10-20 mg sample of mineral was added to a pre-weighed 4 oz polypropylene bottle. Approximately 20 mg of 1,10-phenanthroline and 50 mg of nitrilotriacetic acid (NTA) were added to the bottles. Since ferric iron-NTA complexes are stronger than ferric iron-phenanthroline complexes, NTA was used to complex with ferric iron, allowing only ferrous iron to form a complex with phenanthroline. To dissolve the minerals, 3 mL of 10% H₂SO₄ and 0.5 mL of 48% HF were then added to the bottles. The bottles were placed in a boiling water bath for 30 min. Once removed from the bath, 20 mL of 10% citric acid and 5 mL of 4% boric acid were added. Samples were then diluted to 100-135 mL with Milli-Q water and weighed. The samples were shaken by hand and then divided in half for the total and ferrous iron determinations. Approximately 20 mg of hydroquinone was then added to the samples designated for total iron analysis. All sample bottles were shaken at 350 rpm for 30 minutes, and analyzed on an Hewlett-Packard Model 8451A UV/visible spectrophotometer at 510 nm. Concentrations were determined using ferrous ammonium sulfate standards at 5 calibration levels. This method of iron determination in minerals was tested on a rock standard. The Fe(II) and total Fe contents agreed with the rock standard within 10%.

Wet chemical analysis of the sheet silicates was not conducted for trace metals other than iron. X-ray photoelectron spectroscopy (XPS) conducted on cleavage sheets of the biotite and vermiculite did not show the presence of any redox sensitive trace metals besides iron. Based on a semi-quantitative analysis, the biotite contained <2 wt % Ti. The amount of total iron measured by this semi-quantitative analysis agreed with the iron content obtained from wet chemical analysis for both biotite and vermiculite (Table 1).

Table 1: BET surface area determined by BET and iron content for solids.

Mineral	Specific Surface Area (m ² /g)	Fe(II) Wt. % (g/g)	Fe(III) Wt. % (g/g) ^a
Biotite	1.45	3.1	3.1
Vermiculite	2.94	1.3	0.8
Muscovite	0.75	0.6	1.1
Aerosil 200	200	n.m. ^b	<0.002 ^c
Gibbsite	11.4	d	d
Fresh-ground Pyrite	0.10	n.m.	n.m.
Acid-treated Pyrite	0.11	n.m.	n.m.
Air-exposed Pyrite	0.083	n.m.	n.m.

^a Calculated by difference between total iron and Fe(II).

^b n.m.=not measured.

^c Measured by Degussa, Ridgefield Park, NJ. Speciation not indicated.

^d No iron detected using XPS with detection limit approx. 10% of monolayer (C.J. Papelis, University of Michigan, personal communication).

To study the effect of sulfide on biotite, cleavage sheets of biotite were placed in amber bottles containing deoxygenated Milli-Q water or 0.1 M sulfide. The bottles were sealed with PTFE-lined caps, wrapped with anaerobic tape, and stored in the glovebox. After 6 months, the cleavage sheets were analyzed using XPS to look for changes in the iron speciation and for association of sulfide with the near surface. XPS analysis was conducted on a VG ESCA instrument with a non-monochromatic Al-K α x-ray source and a pass energy of 20 eV. As shown in Figure 1, there was no significant difference in the Fe 2p line shape with biotite treated in an aqueous solution or in a sulfide solution. When adjusted for charge shifting, the Fe 2p peak in Figure 1 corresponds to Fe³⁺ indicating that all of the iron at the near surface of the basal plane is oxidized. A small amount of sulfur was detected at the near surface using XPS (data not shown), but the amount and speciation was not quantifiable. However, the biotite reacted with sulfide had a greyish, metallic luster that was not present on the other biotite sample. SEM photographs (Figures 2 and 3) depict a difference in the two samples: the biotite reacted with sulfide (Figure 3) appears to be more weathered than the biotite reacted in water (Figure 2).

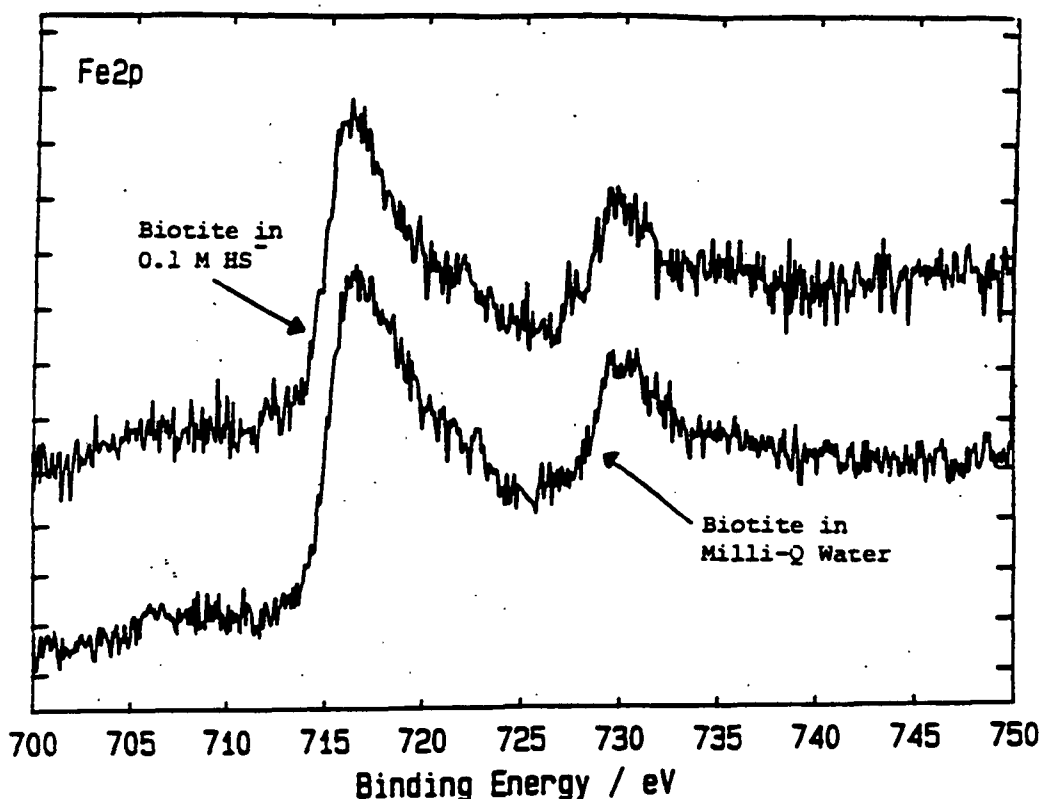


Figure 1: XPS spectra of the Fe 2p peak for biotite reacted for 6 months in anaerobic Milli-Q water and 0.1 M HS⁻. No differences are observed in the oxidation state of iron in the two samples. Peaks are charge shifted by approximately 7.0 eV.

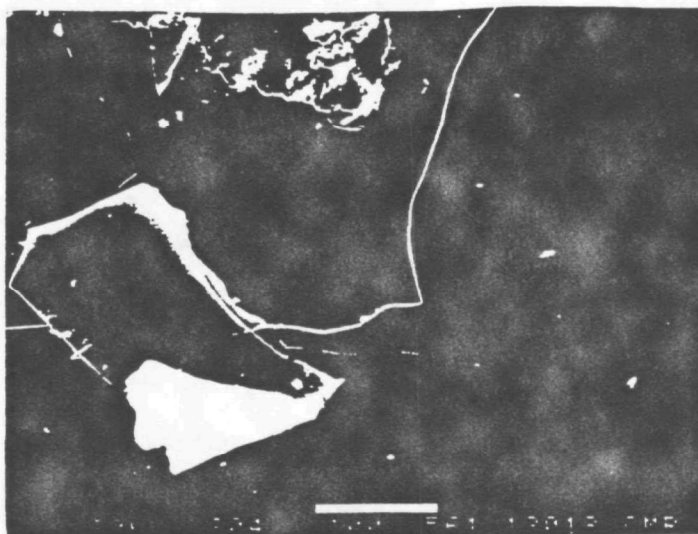


Figure 2: SEM micrograph of biotite cleavage sheet after reaction in anaerobic Milli-Q water for 6 months at 25 °C (white bar equals 100 μ m).

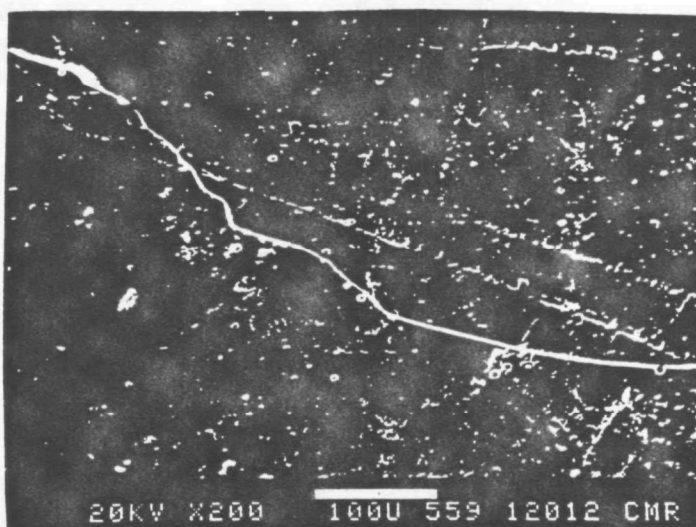


Figure 3: SEM micrograph of biotite cleavage sheet after reaction in 0.1 M HS- for 6 months at 25 °C (white bar equals 100 μ m).

These results show that sulfide does interact with the biotite surface, but the type and extent of effect sulfide has on the surface is unknown. The only studies on the effect of sulfide on weathering or dissolution of minerals has been conducted on iron oxides (Pyzik and Sommer, 1981; dos Santos Afonso and Stumm, 1992; Peiffer et al., 1992). These studies show that sulfide promotes reductive dissolution of iron oxides.

Synthetic Solids Characterization

The only chemical data that we have for Aerosil 200 is from the manufacturer. They do not report the presence of trace metals, except for Ti, which is present at <0.02 wt %. The gibbsite

surface was chemically pure as determined by XPS (C.J. Papelis, University of Michigan, personal communication). The BET surface areas and iron contents for Aerosil 200 and gibbsite are presented in Table 1.

Pyrite Characterization

Single point BET surface area of pyrite was determined using a Micrometrics Flowsorb II 2300 system with 30% N₂/70% He gas mixture. The specific surface areas are summarized in Table 1. The chemical composition of the near-surface of fresh-cleaved pyrite was measured using XPS. The S:Fe ratio was determined to be 2.1. One in ten analyses of reacted pyrite samples showed the presence of 1.1 atomic % Cu.

Kinetic Evaluation of Data

Observed pseudo-first-order rate constants (k'_{obs}) for the disappearance of CCl₄ in the sheet silicate and synthetic solids systems were calculated from regressions of $\ln([CCl_4]_t/[CCl_4]_0)$ vs. time where $[CCl_4]_0$ and $[CCl_4]_t$ were the CCl₄ concentrations at time=0 and time=t, respectively. In the pyrite systems zeroth-order rate constants ($k^0_{CCl_4}$) were calculated from linear regressions of $[CCl_4]_t/[CCl_4]_0$ vs. time wherein $k^0_{CCl_4} = -(\text{slope})/[CCl_4]_0$. At least nine data points were used to determine each rate constant in this study. The standard error of the slope for the linear regression was used to calculate the 95% confidence intervals for the rate constant. In most of the heterogeneous experiments, the 95% confidence intervals were less than 25% of the rate constant. The error was much higher (up to 100%) in the homogeneous experiments because there was relatively little transformation of CCl₄ over the course of the experiment. For experiments with $k'_{obs} < 0.001 \text{ day}^{-1}$, the transformation was considered negligible over the time-period studied and k'_{obs} was assumed to equal zero.

The rate law for the disappearance of CCl₄ in the sheet silicates systems was hypothesized as follows:

$$-\frac{d[CCl_4]}{dt} = k'_{obs}[CCl_4]^\alpha = (k'_{homo} + k'_{hetero})[CCl_4]^\alpha \quad (1)$$

$$= (k_{H_2O} + k_{HS^-} + k'_{hetero})[CCl_4]^\alpha \quad (2)$$

$$= (k_{H_2O} + k_{HS^-}[HS^-]^{\beta_1}[H^+]^{\gamma_1} + k'_{hetero}[HS^-]^{\beta_2}[H^+]^{\gamma_2}[SC]^\delta)[CCl_4]^\alpha \quad (3)$$

where α , β_1 , β_2 , γ_1 , γ_2 , and δ represent the reaction order with respect to reduction in solution and at the mineral interface, k'_{homo} and k'_{hetero} are pseudo-first-order rate constants, and k_{H_2O} , k_{HS^-} and k'_{hetero} are intrinsic rate constants. Eqs. 1, 2 and 3 assume *a priori* that the heterogeneous and homogeneous rate constants are first order with respect to $[CCl_4]$ (e.g. $\alpha=1$). The mineral surface area concentration (SC) was calculated from the product of the solids loading (g/L) and the specific surface area (m²/g) of the mineral. The pK_a for the first dissociation of H₂S at the reaction temperature (Millero, 1986) was used to calculate the HS⁻ concentration based on the pH and the amount of total sulfide added to the system. For homogeneous systems, $k'_{obs} = k'_{homo}$, where k'_{homo} accounts for the reactions with H₂O and HS⁻ in solution. In the heterogeneous systems, $k'_{hetero} = k'_{obs} - k'_{homo}$.

Reaction orders for the different reactants (i.e. HS⁻, pH, CCl₄, SC) were determined by the method of isolation under pseudo-first order conditions. When calculating reaction orders or Arrhenius parameters, individual rate constants (k'_i) were calculated for each data point, i , using the integrated form of a first-order rate law (eq. 4),

$$k_i = \frac{1}{t} \ln \left(\frac{[CCl_4]_0}{[CCl_4]_t} \right), \quad (4)$$

in order to account for the scatter in the original data (Barbash and Reinhard, 1989b). For the heterogeneous systems, k'_{homo} was subtracted from k'_i , yielding a heterogeneous individual rate constant, denoted as $k'_{i,\text{het}}$.

Adsorption

Adsorption of CCl_4 onto biotite and vermiculite was determined by control experiments using radiolabeled CCl_4 at 25 °C. Comparison of the aqueous CCl_4 concentration in the homogeneous and heterogeneous systems over four weeks showed less than 3% adsorption. Because the adsorption of CCl_4 was so small, CCl_4 measurements in the transformation studies were not corrected for adsorption.

SECTION 5

RESULTS AND DISCUSSION

Transformation of CCl_4 by Sheet Silicates

Laboratory studies were conducted to identify and quantify the environmental parameters that govern the transformation rate of CCl_4 in a heterogeneous aqueous environment containing sulfide and sheet silicates (biotite and vermiculite). The parameters studied were temperature, pH, mineral surface area, and sulfide concentration. The reaction rate was hypothesized to be a function of surface area because the reactions have been shown to be faster in the presence of mineral surfaces (Kriegman-King and Reinhard, 1991). Sulfide was also expected to play a role in the kinetics because it could act as either an electron donor or a nucleophile. Data are presented in terms of $[\text{HS}^-]$ instead of total sulfide because HS^- is the dominant species at near-neutral pH, HS^- is a much stronger nucleophile than H_2S (Haag and Mill, 1988; Barbash and Reinhard, 1989a), and HS^- is a stronger reductant than H_2S (Luther, 1990). Lastly, pH dependence was studied because it affects the surface charge of the minerals, the aqueous speciation of sulfide, and probably the surface speciation of sulfide.

Sheet silicates and sulfide were hypothesized to influence the mechanism of CCl_4 transformation in the following ways (Kriegman-King and Reinhard, 1991):

- (1) CCl_4 can undergo electron transfer with ferrous iron in the sheet silicate and the oxidized iron can then be re-reduced by sulfide;
- (2) CCl_4 can react with sulfide that is adsorbed to the sheet silicate; and
- (3) sulfide can react with dissolved iron (released to solution from mineral dissolution) to form a secondary mineral, an iron sulfide, which can then react with CCl_4 .

Structural ferrous iron in biotite has a lower reduction potential than aqueous ferrous iron (White and Yee, 1985). In hypotheses 2 and 3, the adsorbed sulfide or iron sulfide-sulfide can act as an electron donor or as a nucleophile. As far as we know, the reduction potential and/or nucleophilicity of adsorbed sulfide on any solid has not been measured or compared with the reduction potential and/or nucleophilicity of aqueous sulfide. Polysulfides (S_x^{2-} , where x is the number of sulfur atoms) are as strong or stronger nucleophiles than HS^- (Haag and Mill, 1988; Vairavamurthy and Mopper, 1989; Luther, 1990). In these systems, S_x^{2-} may be forming from reaction of HS^- with ferric iron in the sheet silicates. In the pH range of 7-9, S_4^{2-} and S_5^{2-} are the polysulfides that are predicted to be present in solution (Luther, 1990). As a fourth hypothesis, S_x^{2-} may be reacting with CCl_4 via electron transfer or nucleophilic substitution. If secondary mineral formation of pyrite (FeS_2) occurs, the S_2^{2-} group on pyrite may exhibit a reactivity similar to that of the lower polysulfides ($n=2$ or 3), which are slightly less reactive electron donors or nucleophiles than aqueous HS^- (Luther, 1990). However, the iron sulfides, pyrite and marcasite, have been shown to increase the rate of CCl_4 transformation compared with homogeneous rates in systems containing aqueous ferrous iron or HS^- (Kriegman-King and Reinhard, 1991).

Effect of Biotite and Vermiculite on CCl_4 Transformation

Figure 4 shows the effect of biotite ($\text{SC}=55.8 \text{ m}^2/\text{L}$) and vermiculite ($\text{SC}=114 \text{ m}^2/\text{L}$) on the transformation rate of $1 \mu\text{M}$ CCl_4 in the presence of 1 mM HS^- at pH 8.6, 50°C . The average observed rate constants (k'_{obs}) for similar systems are 0.020 ± 0.011 , 0.081 ± 0.005 , and 0.12 ± 0.012

day⁻¹ for the homogeneous, vermiculite, and biotite systems, respectively. The results show that (1) disappearance of CCl₄ is first-order ($\alpha=1$); (2) the minerals increase the transformation rate of CCl₄ over the rate that occurs in homogeneous solution; and (3) biotite is more reactive than

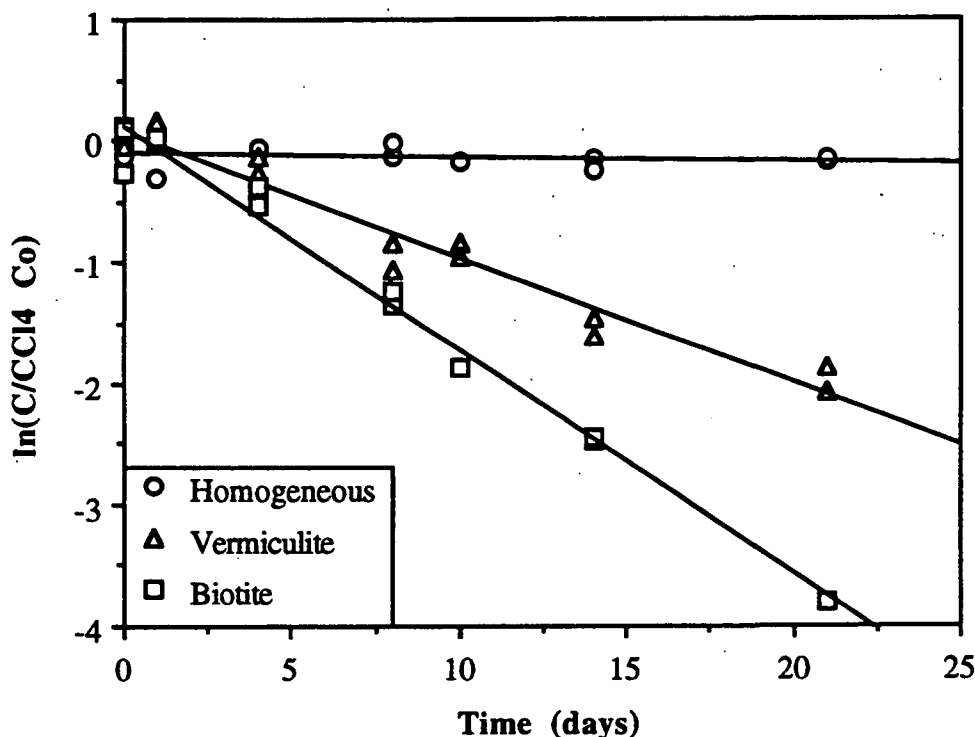


Figure 4: First-order plots of CCl₄ transformation with biotite ($SC_{\text{biotite}}=55.8 \text{ m}^2/\text{L}$) and vermiculite ($SC_{\text{vermic}}=114 \text{ m}^2/\text{L}$), $[\text{HS}^-]=1 \text{ mM}$, $\text{pH}=8.6$ at 50°C .

vermiculite. Jeffers et al. (1989) studied the hydrolysis of CCl₄ in the temperature range of 96-170 °C and also found that the disappearance of CCl₄ was first-order with respect to CCl₄. Using their Arrhenius parameters ($\ln A=36.3 \text{ day}^{-1}$; $E_a=114.5 \text{ kJ/mol}$), the rate of hydrolysis ($k_{\text{H}_2\text{O}}$) of CCl₄ was calculated to be 0.002 day^{-1} at 50°C . Although the rate reported by Jeffers et al. (1989) may be too high because the experiments were conducted in stainless steel tubes that could have promoted the transformation of CCl₄, it is the best hydrolysis data available for CCl₄. In homogeneous systems, the CCl₄ transformation rate in the presence of sulfide is at least an order of magnitude greater than $k_{\text{H}_2\text{O}}$ when $[\text{HS}^-]>0.5 \text{ mM}$. In heterogeneous systems, the CCl₄ transformation rate is faster than $k_{\text{H}_2\text{O}}$ with $[\text{HS}^-]>0.05 \text{ mM}$ and $SC_{\text{biotite}}=55.8 \text{ m}^2/\text{L}$. Even though H₂O is nearly five orders of magnitude more concentrated than HS⁻, HS⁻ is more reactive with CCl₄ than is H₂O. This reactivity is further enhanced in the presence of minerals. These results are not surprising because HS⁻ is a much stronger nucleophile than H₂O or OH⁻ (Swain and Scott, 1953; Haag and Mill, 1988; Barbash and Reinhard, 1989b; Schwarzenbach and Gschwend, 1990) and it may act as a reductant.

CCl₄ Transformation Products

Figure 5 depicts the disappearance of CCl₄ and the appearance of products in a heterogeneous system containing biotite ($SC=55.8 \text{ m}^2/\text{L}$) and 1 mM HS^- . Carbon disulfide (CS₂) was identified as a major intermediate by matching retention times with standard CS₂ solutions on one column using a gas chromatograph equipped with a photoionization detector. As shown

in Figure 6, CS₂ concentrations measured by gas chromatography agree with the "unidentified" volatile fraction calculated by difference between the total volatile fraction determined from ¹⁴C data and the known volatile fractions (CCl₄ and CHCl₃) measured by gas chromatography. About 65% of the CCl₄ was transformed to CO₂ after 60 days. At this time, approximately 20% of the CS₂ was remaining. Chloroform, formed via reductive dehalogenation of CCl₄, reached a maximum of 10%. CHCl₃ was shown to be persistent in these systems by reacting 5 μM CHCl₃ under the same conditions as the CCl₄ experiments. The half-life of CHCl₃ in the presence of 55.8 m²/L biotite and 1 mM HS⁻ at 50°C was measured to be 172 days, whereas the half-life for hydrolysis of CHCl₃ at pH 7.75 and 50°C is 5000 days (Jeffers et al., 1989). Carbon monoxide and a non-volatile component were measured as products in very small quantities (<5% combined) in the CCl₄ systems. The non-volatile product, detected by ¹⁴C fractionation measurements, has not been identified, although Criddle and McCarty (1991) observed the appearance of formate as a major transformation product of CCl₄ in an electrolytic cell.

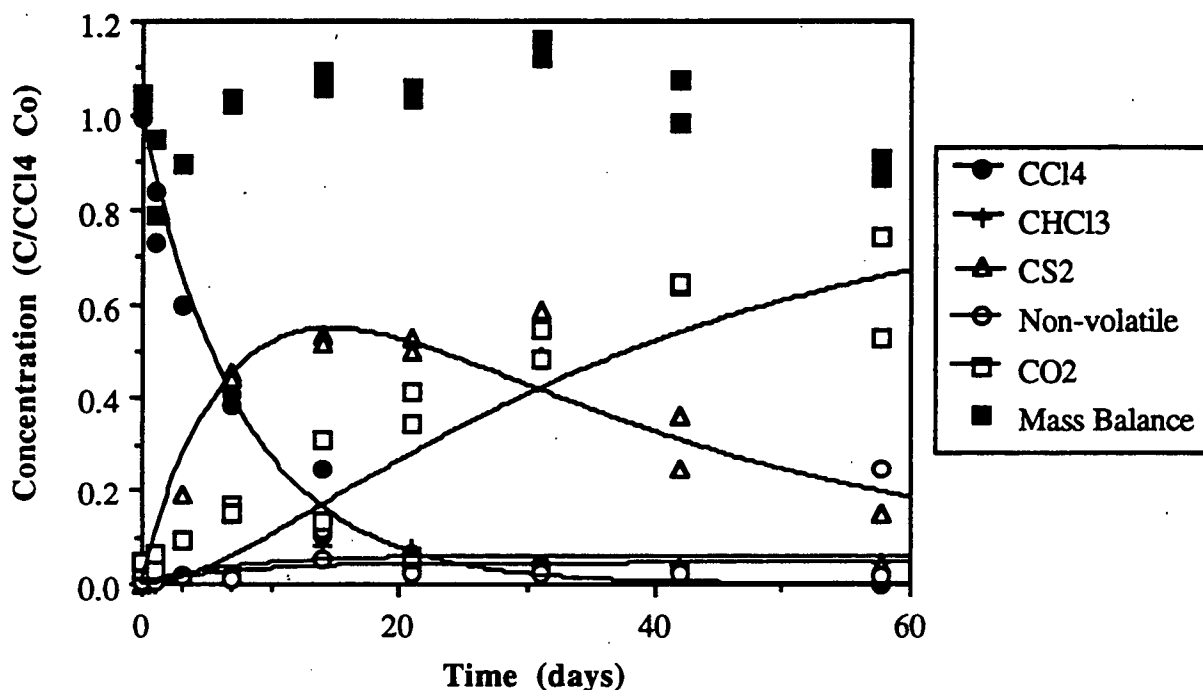


Figure 5: CCl₄ transformation products from reaction with [HS⁻]=1mM, SC_{biotite}= 55.8 m²/L, pH=8.8 at 50 °C. Lines represent best fit using eqs. 8, 12, and 13.

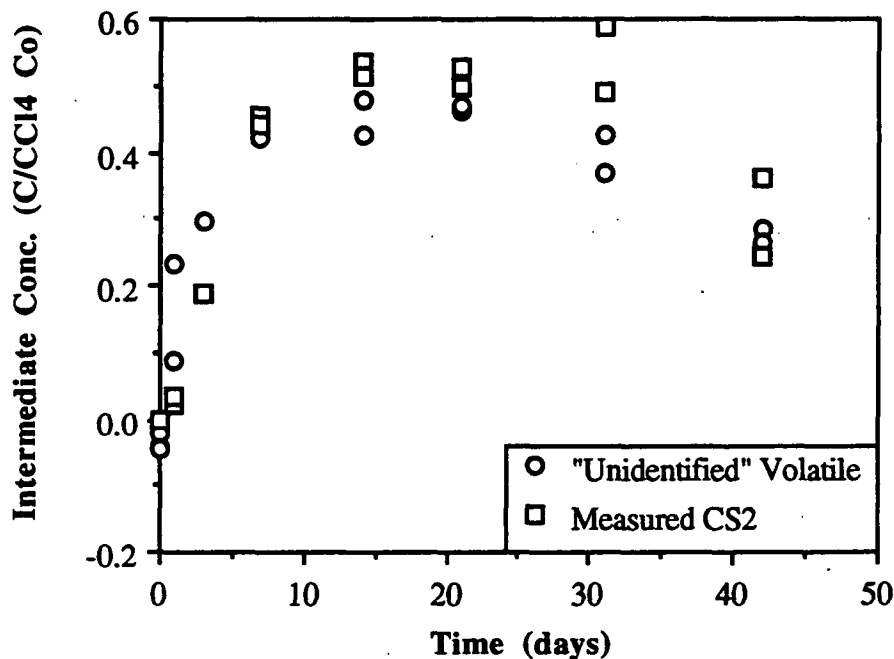
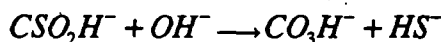
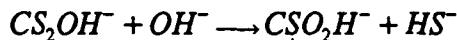
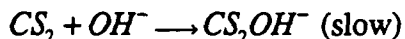


Figure 6: Carbon disulfide (CS₂) was identified as an intermediate of CCl₄ transformation by the agreement between the CS₂ fraction measured by gas chromatography and the "unidentified" volatile fraction measured from ¹⁴C experiments.

The only other known report of CS₂ as a CCl₄ transformation product was observed in systems with fumarate respiring and fermenting *Escherichia coli* (Criddle et al., 1990), although the pathway to form CS₂ from CCl₄ was not known. In the fumarate respiring and fermenting *E. coli* systems, CS₂ was a minor product or intermediate (4.3% and 1.6% of the added CCl₄, respectively). Studies on the hydrolysis and oxidation of CS₂ show that CS₂ is hydrolyzed to CO₂ by hydroxide ion (Hovenkamp, 1963; Adewuyi and Carmichael, 1987). Adewuyi and Carmichael (1987) proposed the following steps for CS₂ hydrolysis:



where the hydrolysis of CS₂ to dithiocarbonate (CS₂OH⁻) is the rate-limiting step. Assuming CS₂ is stoichiometrically converted to CO₂, about 85% of the CCl₄ is ultimately transformed to CO₂ in these systems.

The proposed chemical transformation pathways for CCl₄ under anaerobic conditions are summarized in Figure 7. The products and intermediates in the shadowed boxes were detected in our experiments. As summarized by Criddle and McCarty (1991), the first step for the transformation of CCl₄ has been proposed to be a one-electron reduction to form a trichloromethyl radical and Cl⁻. This radical can follow several different pathways such as additional electron transfer to form a dichlorocarbene and Cl⁻, dimerization to form hexachloroethane, or electron transfer and protonation to produce CHCl₃.

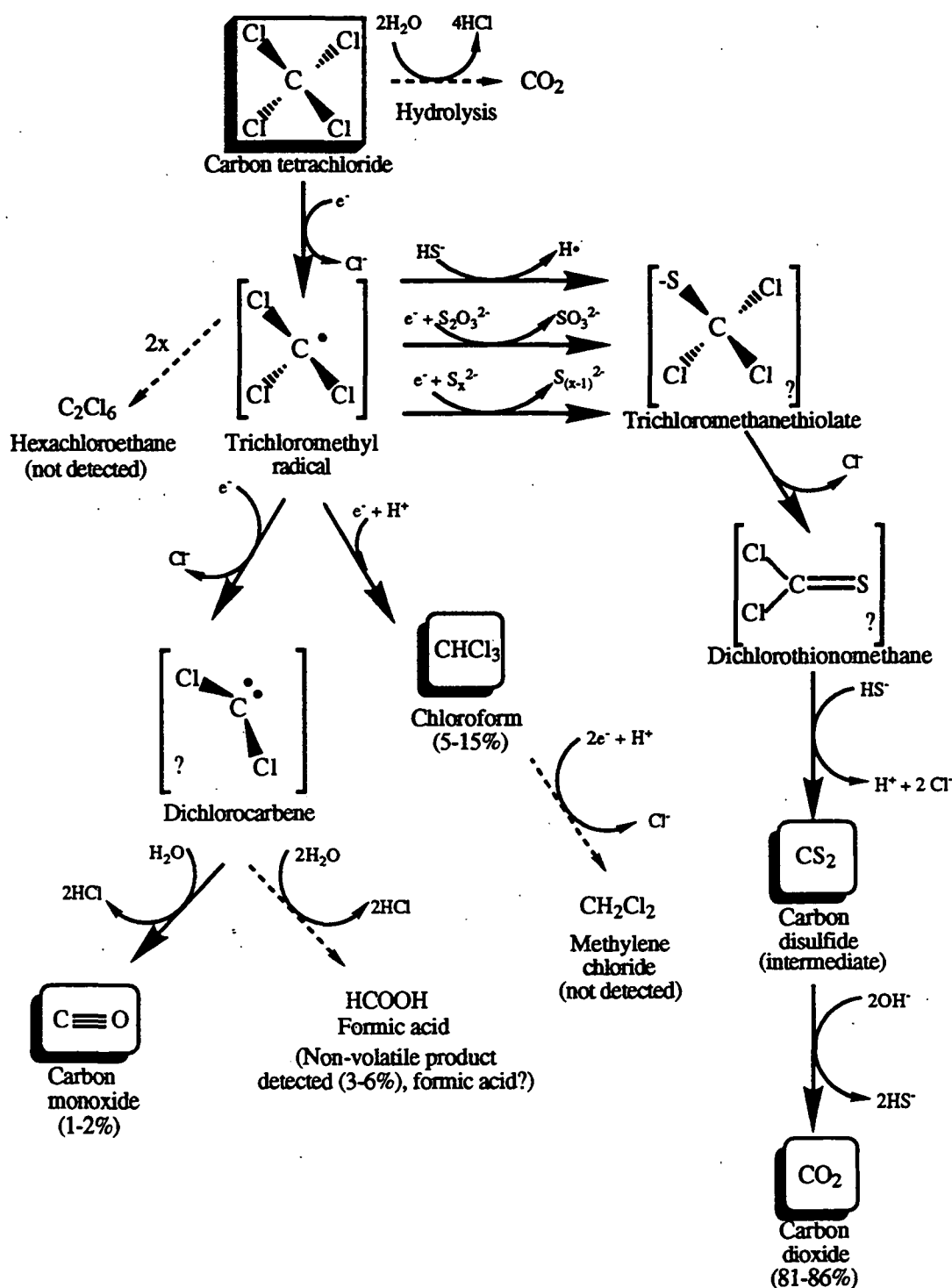


Figure 7: Proposed CCl_4 transformation pathways in HS^- solution containing biotite. Shaded boxes are products and intermediates detected in this study. Compounds in brackets are intermediates proposed from the literature (as cited in Criddle and McCarty, 1991) and this report. Reaction pathways with dashed arrows have been observed in other studies (as cited in Criddle and McCarty, 1991).

The only pathway previously suggested to form CO₂ under anaerobic conditions is direct hydrolysis (Criddle and McCarty, 1991). There has been no evidence that CCl₄ can undergo direct hydrolysis to CO₂, although it is chemically feasible. Jeffers et al. (1989) did not propose a hydrolysis pathway. In our systems, CS₂ appears to be a major intermediate which is transformed to CO₂. The hypothesized pathway to form CS₂ is discussed below.

CCl₄ most likely reacts via an electron transfer reaction to form CCl₄^{•-} which decomposes to a trichloromethyl radical (Shaik, 1983; Pross, 1985a, b). The trichloromethyl radical can react with sulfide or its oxidation products in one of the following ways: (1) it can react with HS⁻ and release H[•]; (2) it can first accept another electron to form the trichloromethyl anion which then reacts with S_x²⁻ or S₂O₃²⁻ to release S_(x-1)²⁻ or SO₃²⁻, respectively; or (3) it can first react with S_x²⁻ or S₂O₃²⁻ producing S_(x-1)²⁻ or SO₃²⁻, respectively, and a trichlorothiomethyl radical which then accepts an electron. These three proposed pathways all result in the formation of trichloromethanethiolate (CCl₃S⁻). S_x²⁻ and S₂O₃²⁻ are likely to be present in these systems by reaction

of HS⁻ and ferric iron in the minerals. The proposed intermediate, CCl₃S⁻, should decompose to form dichlorothionomethane (Cl₂C=S) which reacts with HS⁻ to form CS₂. As discussed above, CS₂ is ultimately hydrolyzed to CO₂ by OH⁻. Rather than reacting with HS⁻ to form CS₂, Cl₂C=S could react with water to form CO₂ via a carbonyl sulfide (COS) intermediate. However, in these systems CS₂, not COS, was formed since the analytical procedure to detect CS₂ could distinguish between COS and CS₂. It should be noted that CS₂ could not be measured in low-sulfide systems (<0.5 mM HS⁻) because the CS₂ hydrolysis rate was faster than the CCl₄ transformation rate.

Rate constants for the different CCl₄ transformation pathways can be evaluated by considering the following relationship:

$$k'_{obs} = k'_{CS_2} + k'_{CHCl_3} + k'_{NV} \quad (5)$$

where k'_{CS₂}, k'_{CHCl₃} and k'_{NV} are pseudo-first-order rate constants that describe the formation of CS₂, CHCl₃, and the non-volatile product, respectively. CO was not measured regularly and was detected in such small quantities that it was not considered in this analysis. To calculate a rate constant for the appearance of CS₂ and its subsequent hydrolysis, the following equation was used:

$$\frac{d[CS_2]}{dt} = k'_{CS_2}[CCl_4] - k'_{CO_2}[CS_2] \quad (6)$$

$$= k'_{CS_2}[CCl_4]_0 \exp(-k'_{obs}t) - k'_{CO_2}[CS_2] \quad (7)$$

where the pseudo-first-order rate constant, k'_{CO₂}, describes the hydrolysis of CS₂. This differential equation can be solved by dividing eq. 7 by eq. 1 and using an integrating factor (Kreyszig, 1983), F, where F=[CCl₄]^{-k'_{CO₂}/k'_{obs}}. The solution is:

$$[CS_2] = \frac{k'_{CS_2}[CCl_4]_0}{(k'_{obs} - k'_{CO_2})} [\exp(-k'_{CO_2}t) - \exp(-k'_{obs}t)] \quad (8)$$

The rate of appearance of CO₂ can be described by eq. 9

$$\frac{d[CO_2]}{dt} = k'_{CO_2}[CS_2] \quad (9)$$

which can be solved for [CO₂] by substitution with eq. 8 and integration.

$$[CO_2] = \frac{k'_{CS_2} [CCl_4]_o}{(k'_{obs} - k'_{CO_2})} \left[(1 - \exp(-k'_{CO_2} t)) - \frac{k'_{CO_2}}{k'_{obs}} (1 - \exp(-k'_{obs} t)) \right] \quad (10)$$

Rate constants for the formation of $CHCl_3$ and the non-volatile product were obtained from eq. 11,

$$\frac{d[CHCl_3]}{dt} = k'_{CHCl_3} [CCl_4] \quad \text{and} \quad \frac{d[Non - vol]}{dt} = k'_{NV} [CCl_4]. \quad (11)$$

These equations were solved for $[CHCl_3]$ and $[Non - vol]$ by substituting CCl_4 with the integrated form of eq. 1 and integrating to obtain

$$[CHCl_3] = \frac{k'_{CHCl_3} [CCl_4]_o}{k'_{obs}} [1 - \exp(-k'_{obs} t)] \quad \text{and} \quad (12)$$

$$[Non - vol] = \frac{k'_{NV} [CCl_4]_o}{k'_{obs}} [1 - \exp(-k'_{obs} t)] \quad (13)$$

The rate constants, k'_{CS_2} , k'_{CO_2} , k'_{CHCl_3} , and k'_{NV} were estimated by fitting the data to eqs. 8, 12, and 13 using both the nonlinear curve-fitting statistical package, SYSTAT (SYSTAT, Inc., Evanston, IL), and the best visual fit. The curve-fitting results for one experiment are shown in Figure 5, and estimated rate constants are contained in Table 2. The curve-fitting results show good agreement across experiments in terms of the fraction of CCl_4 reacting via the three different pathways. Applying eq. 5 to the curve-fitting results, a mass balance of 95-100% was obtained in these experiments.

Temperature Dependence

Since experiments like those shown in Figures 4 and 5 were on the order of weeks to months at 50°C , the temperature dependence of CCl_4 transformation was studied to allow extrapolation of rates to environmentally relevant temperatures. From the temperature data collected at 37.5 , 50.0 and 62.7°C , we calculated values for the Arrhenius activation energy (E_a) and pre-exponential (A) for the homogeneous, vermiculite, and biotite systems. For the heterogeneous systems, the Arrhenius parameters were calculated using the relationship, $k'_{i,het} = k'_i - k'_{homo}$. Calculated E_a and A values are listed in Table 3. Lower E_a values in the heterogeneous systems indicate that these reactions will dominate the homogeneous reactions to an even greater extent at environmentally relevant temperatures. For example, at 50°C , CCl_4 in the presence of biotite and 1 mM HS^- reacts 8 times faster than CCl_4 in the absence of biotite, whereas at 15°C , the biotite system reacts 125 times faster than the homogeneous system.

Table 2: Pseudo-first-order rate constants obtained for CCl₄ transformation pathways using eqs. 8, 12, and 13.

Experiment ^a	k' _{obs}	k' _{CS₂}	k' _{CO₂}	k' _{CHCl₃}	k' _{NV}	Sum ^b
Biotite1	0.185 d ⁻¹	0.15 d ⁻¹	0.06 d ⁻¹	0.022 d ⁻¹	0.003 d ⁻¹	0.175 d ⁻¹
Biotite2	0.129	0.11	0.03	0.006	0.008	0.124
Vermiculite	0.102	0.088	0.035	0.015	0.001	0.104

^a Experiments were conducted with 1 mM HS⁻, 55.8 m²/L biotite or 114 m²/L vermiculite at 50°C. The pH was 8.6, 8.8, and 8.3 for the biotite1, biotite2 and vermiculite experiments, respectively.

^b Sum = k'_{CS₂} + k'_{CHCl₃} + k'_{NV}

Table 3: Arrhenius parameters for CCl₄ transformation with 1 mM HS⁻. E_a and lnA were calculated using k'_{i,het} for biotite and vermiculite and k'_i was used for the homogeneous systems^a.

System	E _a [kJ/mol]	ln(A) [ln(day ⁻¹)]
Homogeneous	122±32 ^b	41.0±2.1 ^a
Vermiculite	91.3±8.4	31.4±0.5
Biotite	59.9±13.3	19.9±0.9

^a Data collected at pH 7.5 and in the temperature range 37.5 - 62.7°C

^b 95% confidence intervals

pH Dependence

The effect of pH on the CCl₄ transformation rate was studied over the pH range of 6-10 at constant HS⁻ concentration (not constant total sulfide concentration). Since several data points of the pH6 and pH10 data were collected at 62.7°C, these rate constants were extrapolated to 50°C assuming that the E_a values tabulated above were independent of pH. The extrapolated data were then combined with other rate constants obtained at 50°C. As shown in Figure 8, in the pH range of 6-10, k'_{homo} and k'_{hetero} did not show a first order pH dependence. In the heterogeneous systems, the rate appears to go through a shallow minimum between pH 7-9. Although the rates appear to increase toward pH 6 and 10, the reaction order of H⁺ does not exceed 0.15. The reason for the higher rates at pH 10 is unknown, but may be due to increased mineral dissolution at this pH. The high experimental error at pH 10 make data interpretation difficult, however. The amount of CHCl₃ produced from CCl₄ also did not vary significantly as a function of pH (data not shown).

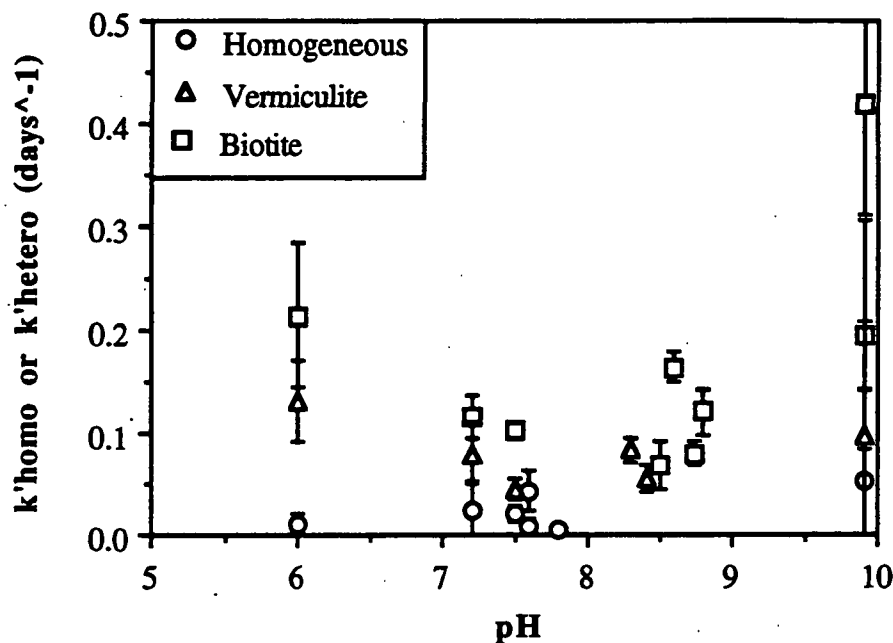


Figure 8: CCl_4 transformation rate at 1 mM HS^- , 50 °C, and 55.8 m^2/L biotite or 114 m^2/L vermiculite in the pH range of 6-10. Error bars are 95% confidence intervals around k'_{homo} or k'_{hetero} .

Effect of Solids Concentration

If the reaction of CCl_4 with HS^- is heterogeneous, k'_{hetero} should be dependent on SC. All of the above experiments were conducted at a biotite surface area concentration ($\text{SC}_{\text{biotite}}$) of 55.8 m^2/L . The effect of $\text{SC}_{\text{biotite}}$ on the CCl_4 transformation rate was measured under conditions ranging from $\text{SC}_{\text{biotite}}=11.2\text{--}280$ m^2/L at constant HS^- concentration (1mM) and $\text{pH}=8\text{--}8.75$. A plot of k'_{hetero} versus $\text{SC}_{\text{biotite}}$ (Figure 9) shows a decreasing slope with increasing $\text{SC}_{\text{biotite}}$. Below 55.8 m^2/L biotite, the data fit a first-order ($\delta=1$) rate law as indicated by the line that passes through the origin. Heterogeneous reactions are typically first-order with respect to the solids concentration (Lasaga, 1984; Stone and Morgan, 1987; Wieland et al., 1988). Above $\text{SC}_{\text{biotite}}=55.8$ m^2/L , the ratio of HS^- to $\text{SC}_{\text{biotite}}$ decreases by a factor of 5. At this lower $\text{HS}^-/\text{SC}_{\text{biotite}}$ ratio, the rate of CCl_4 transformation should be approximately 2.5 times slower (see Effect of Sulfide Concentration and Figure 10). If k'_{hetero} measured for $\text{SC}_{\text{biotite}}=280$ m^2/L is adjusted for the lower $\text{HS}^-/\text{SC}_{\text{biotite}}$ ratio, $k'_{\text{hetero,adjusted}}$ is approximately 0.5 day^{-1} . First-order behavior with respect to $\text{SC}_{\text{biotite}}$ is therefore observed up to 280 m^2/L ($\delta=1$).

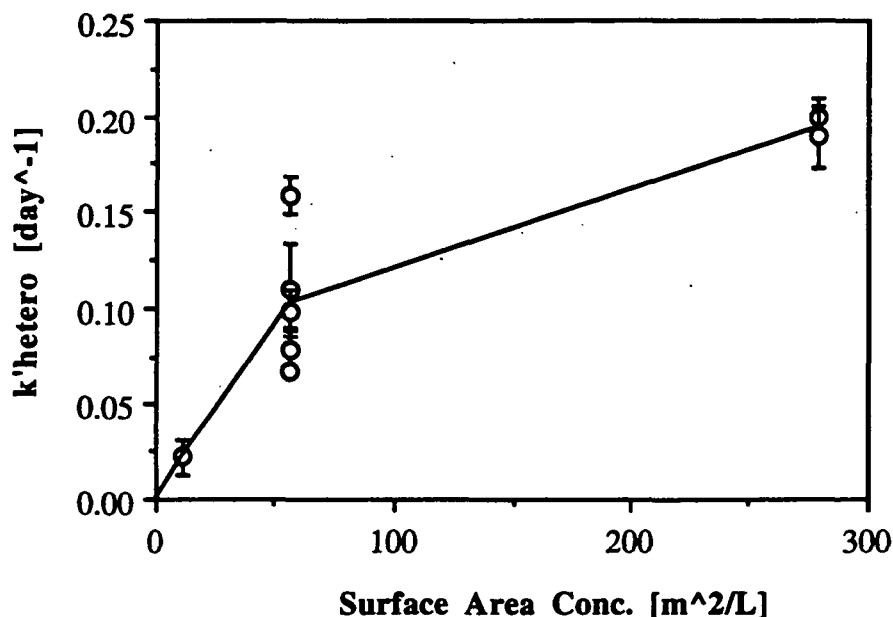


Figure 9: The effect of the biotite surface concentration (SC_{biotite}) on the CCl_4 transformation rate (k'_{hetero} defined eq. 1) at 50°C . The best-fit line for the data at 11.2 and $55.8 \text{ m}^2/\text{L}$ passes through the origin. Error bars are 95% confidence intervals.

Effect of Sulfide Concentration

The effect of HS^- concentration was studied over a range of 0.02–4 mM HS^- at constant SC_{biotite} ($55.8 \text{ m}^2/\text{L}$) and 50°C . The data indicate that above 0.5 mM HS^- , the CCl_4 transformation rate is independent of $[\text{HS}^-]$ (Figure 10). In this range with $\text{pH}=7.5\text{--}8.8$, $k'_{\text{hetero}}=0.10\pm0.01 \text{ day}^{-1}$. Below 0.5 mM HS^- , CCl_4 transformation rate appears to be dependent on HS^- concentration. The CCl_4 systems with 0.02 and 0.05 mM HS^- did not undergo substantial transformation and therefore have a large error associated with them. The reaction order was evaluated using a logarithmic plot of both k'_{hetero} versus $[\text{HS}^-]$ and $k'_{\text{i,het}}$ versus $[\text{HS}^-]$. The data at 0.02, 0.05 and 0.09 mM HS^- could not be corrected for k'_{homo} because the homogeneous rate constants were too small to be measured. The reaction order (β_2) was estimated to be 1.34 and 1.16 ± 0.21 for the k'_{hetero} and $k'_{\text{i,het}}$ methods, respectively. At this point, we assume that the heterogeneous CCl_4 transformation rate is dependent on the HS^- concentration below 0.5 mM, although this dependence is not confirmed. The reaction order (β_1) with respect to HS^- in the homogeneous systems could not be measured under our reaction conditions due to the slow transformation rates in the low sulfide concentration systems. The data conceptually adhere to a Langmuir model sorption/reaction in which rapid sorption at the reactive surface sites precedes the rate-limiting reaction. In this model, the rate increases up to surface site saturation and then becomes independent on the reactant concentration. The data indicated in Figure 10 indicates saturation above 0.5 mM HS^- . However, fitting the data to this model yielded unrealistic Langmuir parameters suggesting that the model assumptions (i.e. uniform surface sites, non interaction of adsorbed molecules) are not appropriate.

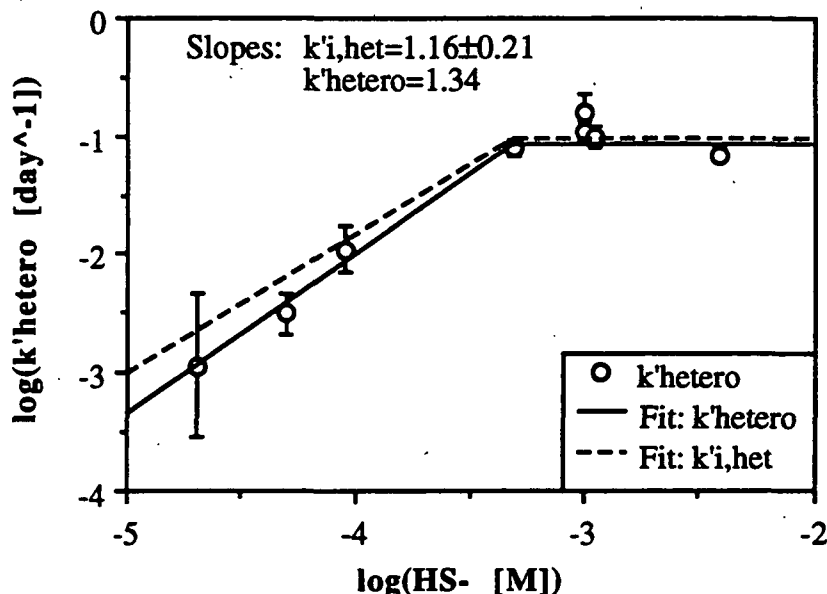


Figure 10: The effect of HS^- concentration on the CCl_4 transformation rate (k'_{hetero}) and the fit to the proposed rate law (Equation 3) with $SC_{biotite} = 55.8 \text{ m}^2/\text{L}$ at 50°C . Above $[HS^-] = 0.5 \text{ mM}$, the rate shows a zeroth-order dependence on $[HS^-]$ ($\beta_2 = 0$). When $[HS^-] < 0.5 \text{ mM}$, β_2 is estimated to be 1.34 or 1.16 ± 0.21 using k'_{hetero} and $k'_{i,hetero}$ data, respectively. Error bars are 95% confidence intervals.

Effect of Ferrous Iron Content

The effect of ferrous iron on the CCl_4 transformation rate was studied by comparing three structurally similar sheet silicates, biotite, vermiculite, and muscovite. Based on an increasing bulk $Fe(II)$ content, the transformation rate increases in the order, muscovite, vermiculite, and biotite (Figure 11). Although ferrous iron appears to play a role in these reactions, the significance of this relationship is not known because (1) iron was measured as a bulk quantity, not as a surface concentration; and (2) the sheet silicates, although being all 2:1 sheet silicates have quite different chemical compositions. Based on rates of potassium release, biotite (White and Yee, 1985) undergoes dissolution significantly faster than muscovite (Knauss and Wolery, 1989). Differences in dissolution rates may explain the observed differences in CCl_4 transformation rates compared with the bulk ferrous iron content.

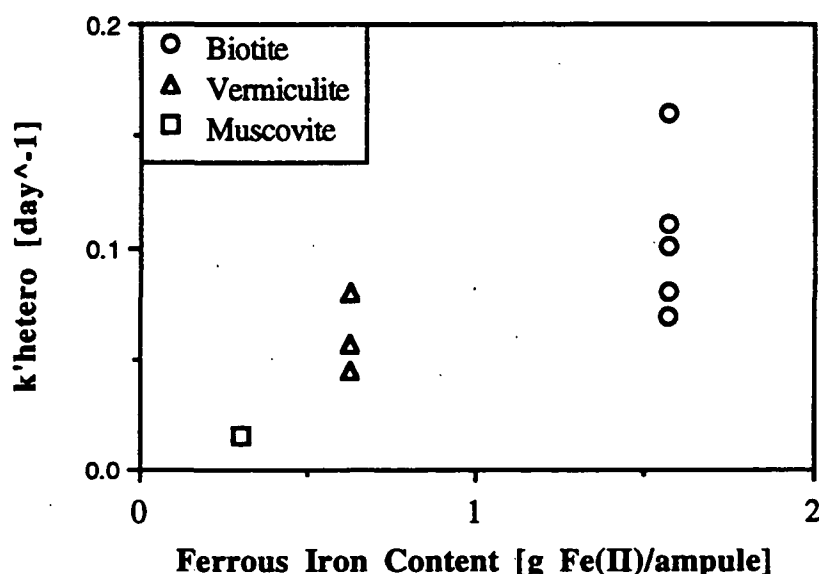


Figure 11: The effect of bulk ferrous iron content in the minerals, muscovite, vermiculite, and biotite on k'_{hetero} at 50 °C.

In the introduction, it was also suggested that S_4^{2-} and S_5^{2-} may be formed by reaction with ferric iron in the sheet silicates. Although these polysulfides should be more reactive with CCl_4 than HS^- or pyrite, there is no relationship between the ferric iron content in the sheet silicates and the CCl_4 transformation rate, suggesting that reaction of CCl_4 with S_x^{2-} is not controlling the transformation rate. In light of the ferrous iron content results and studies of CCl_4 transformation with pyrite and marcasite (results presented in Kriegman-King and Reinhard, 1991 and below), it seems feasible that CCl_4 may be undergoing transformation via reaction with HS^- associated with ferrous iron sites and/or with a secondary iron sulfide phase.

Summary of Sheet Silicate Results

This section shows that HS^- with either biotite or vermiculite increases the CCl_4 transformation rate over rates that occur in homogeneous solution. For the homogeneous reaction at 25°C, the half-life of CCl_4 with 1 mM HS^- was calculated to be 2600 days. In the presence of 1 mM HS^- and vermiculite (114 m²/L) or biotite (55.8 m²/L) 25°C, CCl_4 removal was first order with half-lives of 160 and 50 days, respectively (calculated using the Arrhenius parameters). On a surface area normalized basis, CCl_4 transformation due to the presence of biotite is approximately six times greater than vermiculite.

The results of product studies suggest that reaction the major transformation pathway of CCl_4 with HS^- is via CS_2 to CO_2 . It is proposed that CCl_4 undergoes reduction to form a trichloromethyl radical which then reacts with HS^- , S_x^{2-} , or $S_2O_3^{2-}$ to form CS_2 . The intermediate, CS_2 , hydrolyzes to CO_2 at rates that may be appreciable relative to ground water residence times. At 50 °C, the rate constant for the disappearance of CS_2 ranged from 0.03 to 0.06 day⁻¹. Although Arrhenius constants were not measured for the hydrolysis of CS_2 to CO_2 under reaction conditions herein, literature values for E_a (43.5 kJ/mol--Philipp, 1955 as cited in Adewuyi and Carmichael, 1987); 50.0 kJ/mol--Adewuyi and Carmichael (1987)) result in a hydrolysis rate of 0.006-0.015 day⁻¹ at 25 °C (half-life of 45-110 days) which can be significant

on the scale of ground water transport. About 85% of the CCl_4 is ultimately transformed to CO_2 in these systems. Reductive dehalogenation of CCl_4 to CHCl_3 was observed, although it contributes to only 5-15% of CCl_4 transformation.

Data were presented that showed the effect of temperature, pH, mineral surface area, and sulfide concentration on the CCl_4 transformation rate. At 50 °C, pH 6-9, $\text{SC}_{\text{biotite}}=0-280 \text{ m}^2/\text{L}$ and low HS^- concentrations ($[\text{HS}^-]<0.5 \text{ mM}$), the reaction orders from eq. 3 were determined to be: $\alpha=1$, $\beta_2=1.2$, and $\delta=1$. The pH dependence in the environmentally relevant pH range was too low to be determined reliably and both γ_1 and γ_2 may be assumed to be zero. At high HS^- concentrations ($[\text{HS}^-]=0.5-4 \text{ mM}$) and $\text{SC}_{\text{biotite}}<55.8 \text{ m}^2/\text{L}$, the rate of disappearance of CCl_4 in heterogeneous systems was independent of HS^- concentration ($\beta_2=0$).

Finally, ferrous iron in the sheet silicates appears to be playing a role in the transformation of CCl_4 with HS^- . It is most likely that the reaction is occurring at sites where HS^- is associated with ferrous iron. CCl_4 may also be reacting with iron sulfides formed by iron dissolution and subsequent precipitation with sulfide (Kriegman-King and Reinhard, 1991), but there is no direct evidence from SEM or XPS for iron sulfide formation. Although the mechanism of heterogeneous CCl_4 transformation is unknown, this work clearly shows the significance of mineral surfaces on the transformation rates of a halogenated organic compound compared with homogeneous rates when HS^- is present.

Transformation of CCl_4 by Synthetic Solids

In the previous section, both biotite and vermiculite were shown to react with CCl_4 in the presence of HS^- . It was unclear how the minerals and HS^- increased the transformation rates. The sheet silicates, biotite and vermiculite, are 2:1 sheet silicates that are comprised of an aluminum hydroxide layer (gibbsite) sandwiched between two silicon dioxide (silica) layers. The point of zero charge (pHpzc) of gibbsite is between 8.5 and 10 (Davis and Hem, 1989; Sposito, 1989), and the pHpzc of amorphous silica is approximately 2-3 (Sposito, 1989). Katser and Ropot (1986) studied the adsorption of HS^- on natural sheet silicates and showed that 0.1 g/L slurries of bentonite, hydromica, and palygorskite adsorbed more than 90% of 0.6 mM HS^- within 4 hours. However, no information is available in the literature on the redox properties of sulfide sorbed by mica surfaces. Experiments were conducted with Aerosil 200 (amorphous SiO_2) or gibbsite ($\alpha\text{-Al}(\text{OH})_3$) and HS^- to examine the effect of sheet silicate components that do not contain significant amounts of iron on the CCl_4 transformation rate.

The data presented in Table 4 show that k'_{obs} measured in the presence of gibbsite (5-100 m^2/L) and HS^- did not increase over k'_{obs} measured in homogeneous systems. The Aerosil 200/ HS^- system significantly increased k'_{obs} over homogeneous and gibbsite rates, even when k'_{obs} is normalized for surface area. These data suggest that silica/ HS^- system is capable of promoting the transformation of CCl_4 , rather than the gibbsite/ HS^- system. These results are surprising because one would not expect Aerosil 200, with a pHpzc of 2-3 (Sposito, 1989), to adsorb HS^- . However, Aerosil 200 is a fumed silica with isolated silanol groups that tend not to adsorb water (Burneau and Barres, 1990).

Table 4: Results of CCl₄ transformation in systems containing HS⁻, gibbsite and Aerosil 200 at 50°C.

System	Solids Conc (m ² /L)	pH	[HS ⁻] ^a (mM)	k' _{obs} ^b (day ⁻¹)	Number of Data Points
Homogen.	--	7.2	3.4	0.031±0.022	13
"	--	7.5	1.1	0.021±0.007	11
"	--	7.6	0.88	0.019±0.010 ^c	45 ^c
"	--	8.0	0.95	0.006±0.002	17
" ^d	--	7.7	0.91	0.0052±0.0047	21
Gibbsite	5	8.0	0.95	0.006±0.004	17
"	50	8.4	0.98	0.003±0.002	17
"	100	9.2	1.0	0.007±0.004	17
Aerosil 200	700	7.9	4.5	0.26±0.06	13

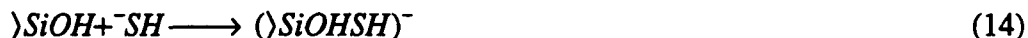
^a[HS⁻] calculated using the pK_a=6.73 at 50°C (Millero, 1986).

^b95% confidence interval around k'_{obs}.

^cAverage of three experiments with 15 data points each.

^dMeasured in the presence of 1 mM Tris buffer.

These isolated groups may be able to adsorb HS⁻ at these sites, even at pH 7-8. The adsorption of HS⁻ at the isolated silanol groups is postulated to be of the form



where sulfide undergoes hydrogen bonding with the silanol surface. Although Aerosil 200 may not be an adequate model of silica surfaces in sheet silicate minerals because of its unusual surface, these results still show that "non-ferrous iron bearing solids" can act as catalysts to promote CCl₄ transformation. It is also conceivable that trace amounts of iron (<0.002 wt %) in the Aerosil 200, rather than the silica surface, were responsible for the transformation of CCl₄ in the presence of HS⁻. A comparison of the reactivity of Aerosil to biotite and vermiculite on a surface area basis shows that Aerosil is not as reactive as the natural sheet silicates.

Transformation of CCl₄ by Pyrite

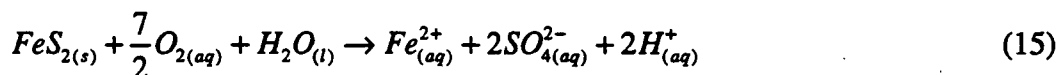
Iron sulfide minerals are ubiquitous in sulfate reducing environments (e.g. Howarth and Teal, 1979; Luther et al., 1982; Lord and Church, 1983; Swider and Mackin, 1989; Huerta-Diaz and Morse, 1992). The iron sulfide minerals pyrite and marcasite were shown to reduce CCl₄ to CHCl₃, but most of the CCl₄ was not accounted for and the reaction mechanism was unknown (Kriegman-King and Reinhard, 1991). Sulfur has been the proposed electron donor in the oxidation of pyrite by different oxidants (Singer and Stumm, 1970; Umaña, 1979; Goldhaber, 1983; Moses et al., 1987; Nicholson et al., 1988; Hyland and Bancroft, 1989, 1990; Mycroft et al., 1990). CCl₄ is proposed to accept an electron from pyrite-sulfur π* (anti-bonding) orbital. The electron is transferred from the π* orbital on the pyrite-S to a σ* (anti-bonding) orbital in CCl₄ which is symmetry allowed according to frontier molecular orbital theory (Luther, 1990). To determine if the reaction is energetically favorable, the energy of the lowest unoccupied molecular orbital (E_{LUMO}) of the oxidant has to be less than or within 6 eV of the energy of the highest occupied molecular orbital (E_{HOMO}) of the electron donor (Luther, 1990). For the case

of CCl₄ and pyrite, E_{LUMO} = -0.28 eV (Shaik, 1983) and E_{HOMO} = -3.9 eV (Luther, 1990) indicating that the reaction is energetically favorable.

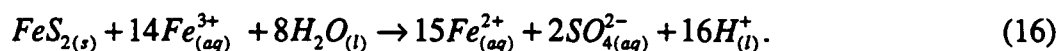
The purpose of this study was to assess the reactivity of CCl₄ with pyrite (FeS₂), specifically to: (1) study the ability of CCl₄ to oxidize pyrite in the presence and absence of O₂ and HS⁻, (2) measure the effect of pretreating the FeS₂ surface with O₂ and acid, (3) determine the CCl₄ transformation products, (4) investigate the effect of reaction conditions on the product distribution, and (5) monitor the aqueous and surface oxidation products of pyrite. Since O₂ is known to oxidize S₂²⁻ groups (Moses et al., 1987; Luther, 1990) and to react with the trichloromethyl radical intermediate (Asmus et al., 1985), both the rates and products of CCl₄ transformation are expected to be influenced by the presence of O₂.

The pyrite treatments and reaction conditions studied were as follows: air-exposed pyrite reacted aerobically, air-exposed pyrite reacted anaerobically, air-exposed pyrite reacted in the presence of sulfide, fresh-ground pyrite reacted anaerobically, and acid-treated pyrite reacted anaerobically. These conditions (except the acid treatment) were chosen to simulate different geochemical scenarios. Although pyrite is formed in anaerobic environments, pyrite is often exposed to aerobic conditions upon weathering (e.g., White et al., 1991). Under oxic conditions, an iron oxide coating will develop on the pyrite surface and will inhibit the reactivity with O₂ (Nicholson et al., 1990) and presumably other oxidants, such as CCl₄. Additionally, O₂ may compete directly with CCl₄ for reaction sites. The extent of competition or inhibition by O₂ and the effect on the CCl₄ product distribution were investigated. Air-exposed pyrite may be re-introduced into an anaerobic or sulfide-rich environment since sulfide is often present in plumes from hazardous waste sites and landfills (Barbash and Reinhard, 1989a). Sulfide may be able to regenerate the pyrite surface through reductive dissolution of the iron oxide coating (Pyzik and Sommer, 1981; dos Santos Afonso and Stumm, 1992; Peiffer et al., 1992). Although fresh-ground pyrite does not necessarily mimic natural unoxidized pyrite because of increases in surface energy induced by grinding (Papirer et al., 1993), it is the best approximation for natural pyrite that has not been exposed to oxygen. Acid-treated pyrite was studied because acid treatment is commonly used in pyrite dissolution and oxidation research to remove high strain areas and to obtain a reproducible surface (Goldhaber, 1983; Taylor et al., 1984; McKibben and Barnes, 1986; Moses et al., 1987; Nicholson et al., 1988). However, the relationship between acid-treated pyrite and *in situ* natural pyrite is also uncertain.

Oxidation rates of pyrite by oxidants such as ferric iron, oxygen, and hydrogen peroxide have been measured under different reaction conditions (Wiersma and Rimstidt, 1984; McKibben and Barnes, 1986; Moses and Herman, 1991). In these studies, the rates of pyrite oxidation were measured either by the disappearance of the oxidant or appearance of sulfate. This indirect method yields accurate results if the stoichiometry of the reaction under consideration is known. Assuming that pyrite-S is oxidized to SO₄²⁻ while the iron redox state is unchanged, the oxidation of pyrite by O₂ and Fe³⁺ can be described by the overall reactions (Moses and Herman, 1991)



and

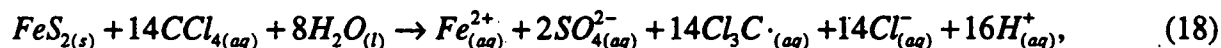


If the appearance of sulfate or the disappearance of ferric iron are used to monitor the rate of pyrite oxidation, then the pyrite oxidation rate equals

$$\text{Rate} = -\frac{d[FeS_2]}{dt} = \frac{1}{2} \frac{d[SO_4^{2-}]}{dt} = -\frac{1}{14} \frac{d[Fe^{3+}]}{dt}. \quad (17)$$

When using SO_4^{2-} to monitor the pyrite oxidation rate, it is assumed that relatively stable intermediates are not formed. The only aqueous sulfur intermediate detected in the oxidation of pyrite at circumneutral pH was $S_2O_3^{2-}$, but its accumulation was negligible (Moses et al., 1987).

The stoichiometry for the oxidation of pyrite by CCl_4 is unknown. Assuming that the oxidation with O_2 and CCl_4 are analogous, we may hypothesize



where 14 moles of CCl_4 react with 1 mole of pyrite to form the intermediate $Cl_3C\cdot$ and sulfate. Under anaerobic conditions with CCl_4 as the only oxidant, pyrite-S may not be fully oxidized to SO_4^{2-} ; partially oxidized sulfur compounds such as polysulfides or thiosulfate may be relatively stable. This equation also assumes that CCl_4 is reduced only to $Cl_3C\cdot$; whereas for formation of $CHCl_3$, CO , or $HCOOH$, two electrons are required resulting in a stoichiometric coefficient of 7 rather than 14, thereby doubling the pyrite oxidation rate. By monitoring the disappearance of CCl_4 , we can use a stoichiometric coefficient of 14 to provide a low estimate of the pyrite oxidation rate, thus enabling us to compare the reactivity of pyrite with CCl_4 and other oxidants.

Effect of Pyrite Pretreatment on CCl_4 Transformation Rate

In order to establish the reaction kinetics for the disappearance of CCl_4 with 1.2 m² pyrite, the data were fit to both a first- and a zeroth-order reaction model. Rate constants were obtained for the first- and the second-order models were obtained from the slopes of semi-logarithmic plots of $[CCl_4]/[CCl_4]_0$ versus time and linear plots of $[CCl_4]/[CCl_4]_0$ versus time, respectively. An example of the results of the kinetic model fits for the O_2 -Exp/Aer and Acid/An experiments are depicted in Figure 12. The data showed a much better adherence to zeroth-order model than to the first-order model. A poor fit was found for the fresh-ground system ($R^2 = 0.65$) presumably due to heterogeneous nature of the freshly cleaved surfaces.

A zeroth-order dependence on oxidant concentration is expected when a heterogeneous reaction is chemically controlled, rather than diffusion controlled (Goldhaber, 1983). Rate constants for the disappearance of CCl_4 ($k^0_{CCl_4}$) are shown in Table 5. The rate constants were normalized by the pyrite surface concentration, assuming the reaction was first-order with respect to the surface concentration, SC (Lasaga, 1981; Moses and Herman, 1991), according to the equation

$$\frac{d[CTET]}{dt} = -k^0_{CCl_4} [SC] \quad (19)$$

where SC is the product of the specific surface area of the solid [m²/g] and the solids loading [g/L].

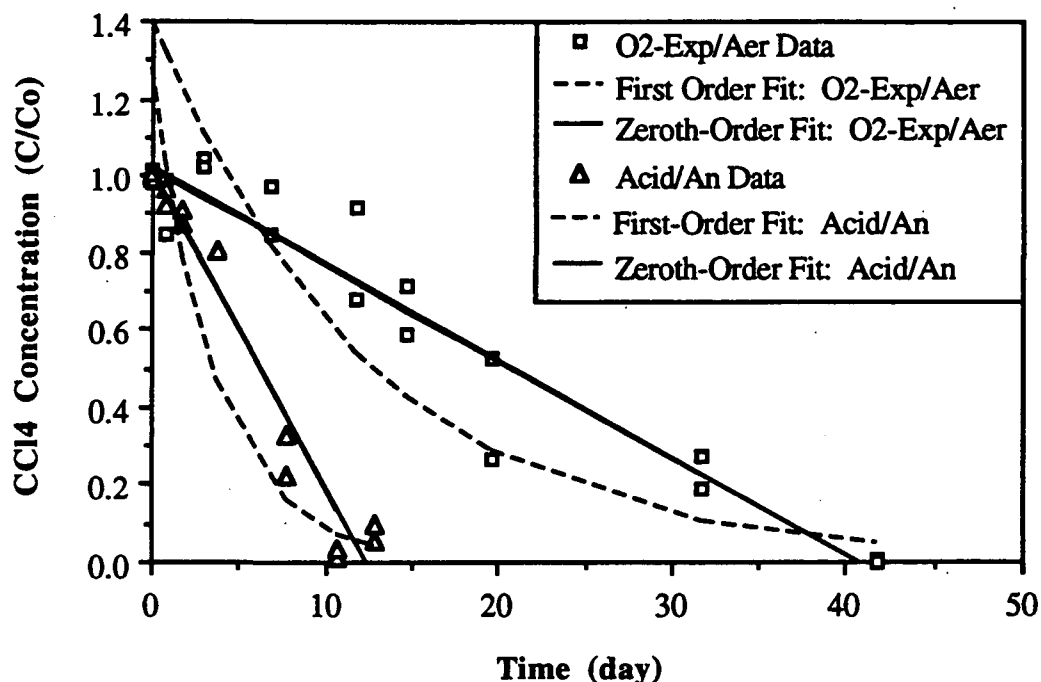


Figure 12: Disappearance of CCl_4 in the presence of air-exposed pyrite reacted under aerobic conditions and acid-treated pyrite reacted under anaerobic conditions at 25 °C. Data are fit with both first- and zeroth-order kinetic models.

Table 5: Zeroth-order rate constants for CCl_4 transformation with pyrite (1.2-1.4 m^2/L) reacted under aerobic and anaerobic conditions at 25 °C.

Pyrite Conditions	Slope (d^{-1})	R^2	$k^0 \text{CCl}_4$ ($\text{mol}/\text{m}^2 \cdot \text{d}$)	95% Confidence Interval
Air-exposed, Aerobic	0.025	0.93	0.021	0.017-0.026
Air-exposed, HS^-	0.031	0.87	0.026	0.020-0.032
Air-exposed, Anaerobic	0.057	0.85	0.047	0.035-0.049
Fresh-Ground	0.056	0.65	0.039	0.022-0.056
Acid-Pretreated	0.082	0.96	0.053	0.046-0.060

In the acid-treated pyrite system, >90% of 1 μM CCl_4 was transformed within 12 days at 25 °C, whereas half-lives in homogeneous solution are 1400 days for 1 mM HS^- at 25 °C and 105 days for 0.1 mM $\text{Fe}^{2+}_{\text{aq}}$ at 50 °C (Kriegman-King, 1993). Assuming an activation energy of 60-120 kJ/mol, the half life of CCl_4 with 0.1 mM $\text{Fe}^{2+}_{\text{aq}}$ at 25 °C ranges from 700-4500 days. The aqueous Fe^{2+} and HS^- concentrations in suspensions of pyrite in deoxygenated Milli-Q water have recently been measured to be approximately 0.1 mM, in a 1:2 ratio, respectively (L. Rönngren and S. Sjöberg, University of Umeå, Sweden, personal communication, 1993), suggesting that the solubility product of pyrite is higher than reported previously. The CCl_4

transformation rates that were measured in the Fe^{2+} and HS^- aqueous systems were at concentrations that would be expected in the pyrite systems. The rate data therefore support a surface-controlled reaction mechanism for the transformation of CCl_4 by pyrite because (1) zeroth-order kinetics were observed and (2) the reaction with pyrite was much faster than in homogeneous solutions. Over longer time periods, however, the reaction may become diffusion controlled when an iron oxide coating forms on the pyrite and the oxidant and products have to diffuse through the oxide coating (Goldhaber, 1983; Nicholson et al., 1990).

In Table 5, the data show that CCl_4 reacts the fastest with the acid-treated pyrite, although the air-exposed pyrite reacted anaerobically is not statistically slower. As expected, the slowest transformation rate was observed when CCl_4 was reacted with pyrite under aerobic conditions. However, the rate constant was only 2.5 times slower than the acid-treated system. The large error associated with the fresh-ground pyrite system precludes comparison with other rate constants. The stresses induced by grinding (Papirer et al., 1993), however, may still be responsible for the scatter in the fresh-ground/anaerobic system. This heterogeneity was likely removed during pretreatment by O_2 or acid.

The rate constants are compared to rates of pyrite oxidation by O_2 , Fe^{3+} , and H_2O_2 in Table 6. In order to compare pyrite oxidation rates by CCl_4 to rates by other oxidants, it is assumed that CCl_4 oxidizes pyrite-S to SO_4^{2-} . Using eq. 18, the molar pyrite oxidation rate is 1/14 the CCl_4 disappearance rate. When the pyrite oxidation rate is calculated from the disappearance rate of CCl_4 , competing reactions by other oxidants such as O_2 are not accounted for. Although solution conditions and pretreatments differ, it is clear that CCl_4 reacts with pyrite as fast or faster than O_2 and Fe^{3+} (Table 6).

Table 6: Comparison of pyrite oxidation rate by CCl_4 with literature rates of oxidation by O_2 , Fe^{3+} , and H_2O_2 at room temperature.

	Pretreatment	pH	Oxidant	Oxidation Rate [nmol/m ² ·s]
This work	Air-exposure	6.5	CCl_4 , O_2	15 ^{a,b}
	Air-exposure	6.5	CCl_4	45 ^a
	Mild HCl Wash	6.5	CCl_4	70 ^a
Moses and Herman (1991)	Boiling HCl Wash	6.0	Fe(III)	10
	"	6.0	O_2	1
	"	6.0	O_2 , Fe(III)	0.5
McKibben and Barnes (1986)	Mild HNO_3 Wash	2.0	Fe(III)^c	5
	"	2.0	O_2^c	500
	"	2.0	H_2O_2^c	2×10^6
Wiersma and Rimstidt (1984)	None	2.0	Fe(III) , O_2	10

^a Assumes a stoichiometry of 14 moles of CCl_4 reduced to Cl_3C^- for 1 mole of pyrite oxidized to SO_4^{2-} .

^b Represents pyrite oxidation rate due to CCl_4 , not the total rate due to both O_2 and CCl_4 .

^c Did not observe zeroth-order dependence for oxidants. Used 0.3 mM oxidant concentration to calculate rate.

In environmental situations where CCl_4 will likely be present with O_2 and Fe^{3+} , pyrite oxidation by CCl_4 will not be necessarily inhibited or out-competed by O_2 and Fe^{3+} . Hydrogen

peroxide reacts with pyrite orders of magnitude faster than CCl_4 , O_2 , or Fe^{3+} . However, an oxide coating will develop, and with time, the reactivity of the pyrite surface toward CCl_4 , or any oxidant, will eventually become diffusion controlled (Nicholson et al., 1990).

Reaction of air-exposed pyrite in the presence of sulfide shows that treatment of an oxidized pyrite surface with HS^- does not restore the reactivity of pyrite. Rather, sulfide appears to inhibit the transformation of CCl_4 by pyrite, even relative to the air-exposed/anaerobic pyrite system. At pH 7.75, 85% of the sulfide is present as HS^- ; and more than 100 μM is present as H_2S . Because of the observed zeroth-order dependence on CCl_4 , reaction sites on pyrite are inferred to be saturated with CCl_4 when $[\text{CCl}_4]=1\mu\text{M}$ and $[\text{H}_2\text{S}]$ is 100 times more concentrated than CCl_4 , it is conceivable that H_2S blocks CCl_4 reaction sites. Characterization of the pyrite surface chemistry is necessary to understand the interaction of sulfide species with the pyrite surface.

CCl_4 Transformation Products

As shown in Table 7, the CCl_4 product distribution varies greatly depending on the reaction conditions even though $k^0_{\text{CCl}_4}$ only varies by a factor of 2.5.

Table 7: CCl_4 product distribution from reaction with pyrite under aerobic and anaerobic conditions at 25 °C.

Condition (Time) ^a	CCl_4	CHCl_3	CS_2	CO_2	Formate ^b	Adsorbed ^c	Mass Balance ^d
Air-exposed; Aerobic (42 d)	0-1%	5-6%	11-15%	52-59%	2%	10% (2%NV 8% CO_2)	84-87%
Air-exposed, HS^- (31 d)	0-10%	21-22%	NM ^e	NM	NM	NM	NM
Air-exposed, Anaerobic (20 d)	0-1%	28-30%	0-3%	26-30%	7-9%	12% (7%NV 5% CO_2)	82-84%
Fresh-Ground (13 d)	1%	48%	2%	10%	5%	12% ^f	78%
Acid-Pretreated (13 d)	6-10%	20-21%	19-20%	17%	4%	9% (2%NV 7% CO_2)	78%

^a Reaction time in days is in the parentheses.

^b Formate was not directly measured in these experiments. The formate concentration was assumed to equal the non-volatile concentration measured using ^{14}C analysis.

^c Adsorbed amount does not account for volatile compounds adsorbed. NV=non-volatiles.

^d Mass balance of aqueous volatile compounds was obtained in all cases. Total radioactivity in solution + adsorbed non-volatile and CO_2 fractions are equal to the mass balance within 5%. Missing fraction likely to be adsorbed volatiles.

^e NM=not measured.

^f Breakdown of adsorbed products not measured.

Under aerobic conditions, the major product was CO_2 (60-70%). Including the hydrolysis of CS_2 to CO_2 (Adewuyi and Carmichael, 1987; Kriegman-King and Reinhard, 1992), CO_2 accounts for 70-80% of the CCl_4 transformed. In contrast, the fresh-ground pyrite system forms approximately 50% CHCl_3 and ultimately only 10-20% CO_2 . The total CO_2 amount in the fresh-ground system is a rough estimate because the speciation of the adsorbed fraction was not measured. Interestingly, some CS_2 was formed in all systems suggesting that the CCl_4 or reactive intermediates react with S_2^{2-} sites on pyrite, even in the presence of O_2 . The volatile fraction measured from scintillation counting agreed with the sum of the CCl_4 , CHCl_3 , and CS_2 fractions, that CO and C_2Cl_6 are not formed in these systems. A loss in total radioactivity from solution as a function of time suggests that a fraction of the CCl_4 or its transformation products is adsorbed to pyrite. Assuming the method to measure adsorbed CO_2 and HCOOH is valid, it is likely that the missing fraction is a compound that is volatile when desorbed and is not detected with our experimental methods.

In an experiment conducted anaerobically with $100\ \mu\text{M}$ CCl_4 and $1.2\ \text{m}^2/\text{L}$ pyrite, the appearance of formate was monitored. As shown in Figure 13, after disappearance of 95% of the CCl_4 , approximately $4\text{-}6\ \mu\text{M}$ formate was detected, accounting for 4-6% of the initial CCl_4 concentration. For comparison, in ^{14}C -labeled CCl_4 experiments, approximately 5% of the CCl_4 is transformed to a non-volatile product when reacted with pyrite anaerobically (Table 7). The direct measurement of formate by ion chromatography and its agreement with the fraction of non-volatile products measured by scintillation counting agree with the above assumption that the non-volatile compound is formate.

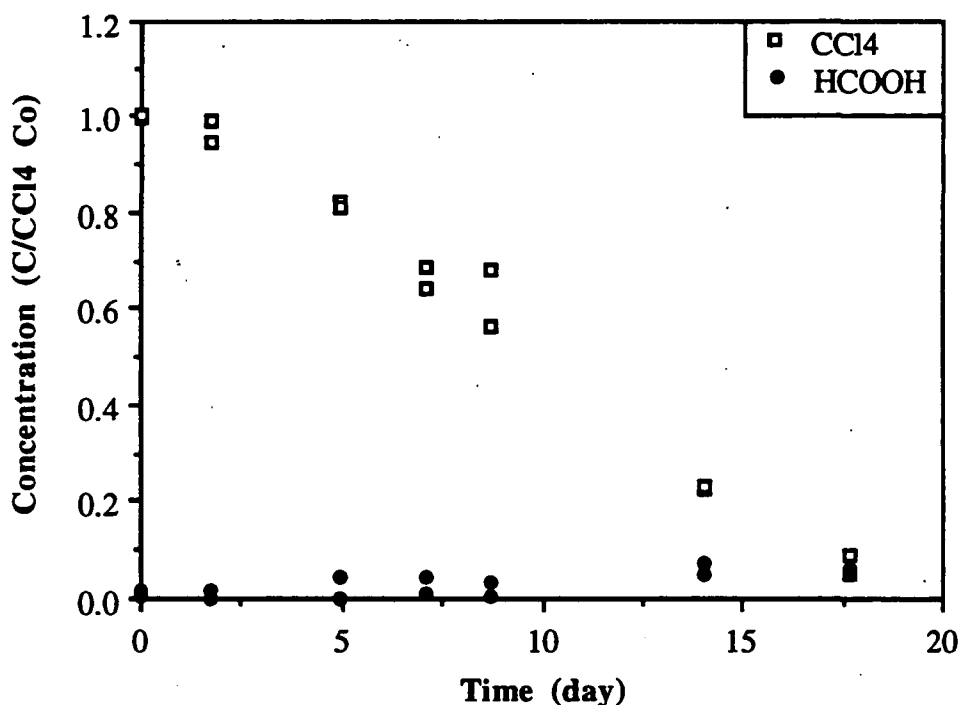


Figure 13: The disappearance of $100\ \mu\text{M}$ CCl_4 with $1.2\ \text{m}^2/\text{L}$ pyrite reacted anaerobically at $25\ ^\circ\text{C}$. Appearance of formic acid was measured with an ion chromatograph.

Air-Exposed Pyrite/Aerobic--

Using the product data as a function of time, the rate constants for the formation of the products can be estimated. Because the disappearance of CCl_4 was zeroth order, the appearance of the products is also assumed to be zeroth order except when secondary products are formed that require more complex rate laws. The rate constants for the appearance of CHCl_3 and HCOOH (k'_{CHCl_3} and k'_{NV} , respectively) were calculated assuming a zeroth-order rate law (Table 8). Under aerobic conditions, CO_2 can form via hydrolysis of CS_2 (Kriegman-King and Reinhard, 1992) or via reaction of O_2 with the trichloromethyl radical (Asmus et al., 1985). If any CO_2 is formed via hydrolysis of CS_2 , then the appearance of CO_2 cannot be modeled by a zeroth-order equation. Assuming CO_2 is formed only by the CS_2 pathway, eqs. 20 (a, b) can be used to solve for $[\text{CS}_2]$ and $[\text{CO}_2]$ as a function of time.

$$\frac{d[\text{CS}_2]}{dt} = k_{\text{CS}_2}^{\circ} - k'_{\text{CO}_2}[\text{CS}_2] \quad (\text{a}) \quad \text{and} \quad \frac{d[\text{CO}_2]}{dt} = k'_{\text{CO}_2}[\text{CS}_2] \quad (\text{b}) \quad (20 \text{ a, b})$$

where $k_{\text{CS}_2}^{\circ}$ is a zeroth-order rate constant for the appearance of CS_2 and k'_{CO_2} is a first-order rate constant for the formation of CO_2 . Using SYSTAT (SYSTAT, Inc, Evanston, IL), the CS_2 data were fit with the equation

$$[\text{CS}_2] = \frac{k_{\text{CS}_2}^{\circ}}{k'_{\text{CO}_2}} (1 - \exp(-k'_{\text{CO}_2} t)) \quad (21)$$

to solve for the rate constants, $k_{\text{CS}_2}^{\circ}$ and k'_{CO_2} (Table 8). These constants were then substituted

Table 8: Rate constants for the disappearance of CCl_4 and appearance of intermediates and products from reaction with pyrite under aerobic and anaerobic conditions at 25 °C.

Rate Constant ^a	Air-exposed Pyrite Reacted Aerobically		Acid-treated Pyrite Reacted Anaerobically	
	No Interm. ^b $R^2_{\text{adj}}=0.78^d$	Intermediate ^c $R^2_{\text{adj}}=0.85$	No interm. ^b $R^2_{\text{adj}}=0.85$	Intermediate ^c $R^2_{\text{adj}}=0.85$
$k_{\text{CCl}_4}^{\circ}$ [mol/m ² · d]	0.021	0.021	0.053	0.053
k_i° [mol/m ² · d]	--	0.020	--	0.023
$k_{\text{CS}_2}^{\circ}$ [mol/m ² · d]	0.0078	--	0.022	--
k'_{CS_2} [L/m ² · d]	--	0.012	--	7.7
k_{CO_2} [L/m ² · d]	0.040	0.012	0.12	0.12
$k_{\text{CHCl}_3}^{\circ}$ [mol/m ² · d]	0.00092	0.00092	0.012	0.012
k_{NV}° [mol/m ² · d]	0.00040	0.00040	0.0027	0.0027

^a k° = zeroth-order rate constant; k' = first-order rate constant. Symbols are defined in text.

^b $\text{CCl}_4 \rightarrow \text{CS}_2 \rightarrow \text{CO}_2$

^c $\text{CCl}_4 \rightarrow \text{Int} \rightarrow \text{CS}_2 \rightarrow \text{CO}_2$

^d R^2_{adj} accounts for the number of fitting parameters.

than was measured, suggesting that CO_2 is formed via the reaction of $\text{CCl}_3\cdot$ with O_2 . However, the curve for the appearance of CS_2 also does not fit the data well ($R^2_{\text{adjusted}}=0.78$). There is a time lag before $[\text{CS}_2]$ starts to increase, suggesting formation of a relatively stable intermediate in the path to form CS_2 .

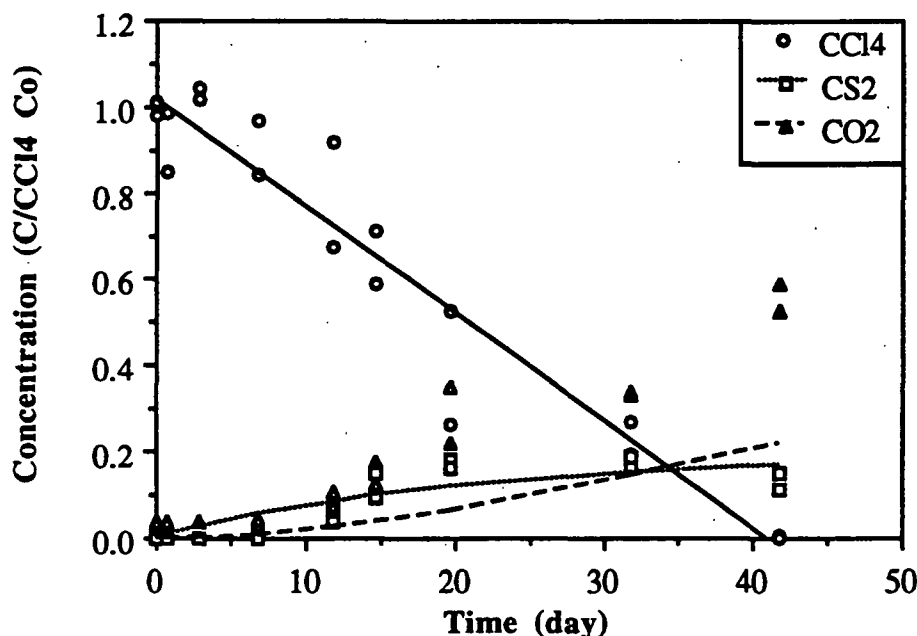


Figure 14: Disappearance of CCl_4 in the presence of pyrite under aerobic conditions at 25 °C. Appearance of the products, CS_2 and CO_2 , with model results assuming the only path to form CO_2 is $\text{CCl}_4 \rightarrow \text{CS}_2 \rightarrow \text{CO}_2$.

If it is hypothesized that a stable intermediate is formed, then the appearance of CS_2 can be modeled using the equations,

$$\frac{d[\text{Intermed.}]}{dt} = k_1^0 - k_{\text{CS}_2} [\text{Intermed.}] \quad (22)$$

$$\frac{d[\text{CS}_2]}{dt} = k_{\text{CS}_2} [\text{Intermed.}] - k_{\text{CO}_2} [\text{CS}_2] \quad (23)$$

where k_1^0 is the zeroth-order rate constant for the formation of the intermediate. In eqs. 22 and 23, the rate constant for the appearance of CS_2 (k_{CS_2}) is now assumed to be first order. Using the solution to eq. 22 which is of the same form as eq. 21, eq. 23 can be solved to give the CS_2 concentration,

$$[\text{CS}_2] = \frac{k_1^0}{k_{\text{CO}_2} - k_{\text{CS}_2}} \left(\frac{k_{\text{CS}_2}}{k_{\text{CO}_2}} \exp(-k_{\text{CO}_2} t) - \exp(-k_{\text{CS}_2} t) \right) + \frac{k_1^0}{k_{\text{CO}_2}} \quad (24)$$

The curve-fitting results obtained from eq. 24 are shown in Table 8 and Figure 15. There is an improvement in the CS₂ fit ($R^2_{\text{adjusted}}=0.85$), and the CO₂ data are also fit quite well. The curve predicts formation of 5-10% more CO₂ than was measured in solution which might correspond to the 8% CO₂ adsorbed. The appearance of the hypothetical intermediate is also included in Figure 15. At the end of the experiment, the model predicts that the intermediate attains a steady-state concentration of approximately 15% which agrees with the missing mass balance (Table 7).

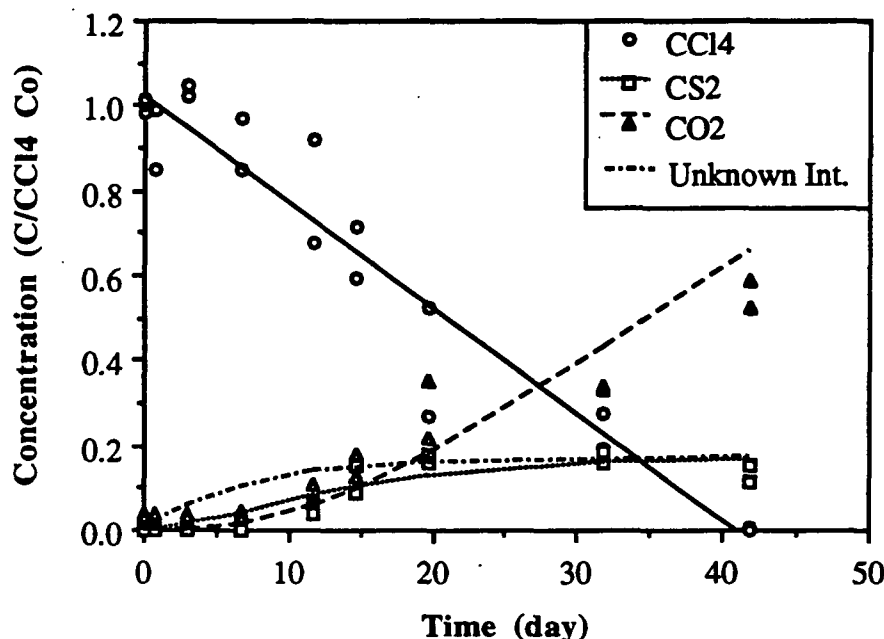


Figure 15: Disappearance of CCl₄ in the presence of pyrite under aerobic conditions at 25 °C. Appearance of the products, CS₂ and CO₂, with model results assuming the only path to form CO₂ from CCl₄ is: CCl₄ → Intermed. → CS₂ → CO₂.

Acid-Treated Pyrite/Anaerobic--

A similar fitting analysis was conducted on the results from the acid-treated pyrite system. In this case, no significant difference in the CS₂ fit was observed if the appearance of an unknown intermediate was included. As shown in Table 8, the rate constant for the disappearance of the unknown intermediate I (k_I') is relatively large, indicating that the intermediate I is very short-lived. Therefore, k_I' is thus approximately equal to the rate constant for the appearance of CS₂ (k_{CS_2}'). In Figure 16 the predicted CO₂ concentrations do not accurately describe the measured CO₂ within the analytical precision of $\pm 5\%$. The CO₂ data do not have a lag; CO₂ appears to form without a stable intermediate. Although the over-predicted CO₂ concentrations again likely correspond to the adsorbed CO₂ (Table 7), the measured CO₂ do not have a lag; CO₂ appears to form independently of CS₂ hydrolysis through a yet unidentified pathway.

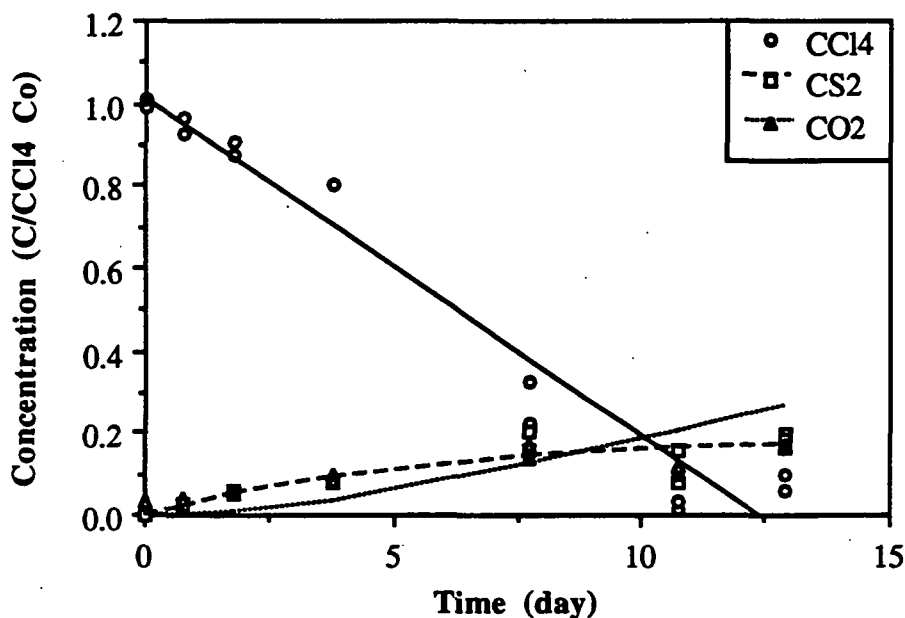


Figure 16: Disappearance of CCl_4 in the presence of acid-treated pyrite under anaerobic conditions at 25 °C. Appearance of the products, CS_2 and CO_2 , with model results assuming the only path to form CO_2 is: $\text{CCl}_4 \rightarrow \text{CS}_2 \rightarrow \text{CO}_2$.

Pyrite Oxidation Products

Aqueous Sulfur Oxidation Products--

The presence and absence of CCl_4 did not affect the aqueous sulfate concentrations (data not shown). In an experiment in which pyrite was reacted anaerobically with 100 μM CCl_4 , consistent formation of 2-4 μM $\text{S}_2\text{O}_3^{2-}$ was observed. The control, reacted in the absence of CCl_4 , contained only a sporadic appearance of $\text{S}_2\text{O}_3^{2-}$ at $<3 \mu\text{M}$. These data suggest that $\text{S}_2\text{O}_3^{2-}$ is an intermediate or product formed during oxidation of pyrite by CCl_4 . $\text{S}_2\text{O}_3^{2-}$ presumably reacts with CCl_4 or CCl_4 transformation intermediates until it is fully oxidized to SO_4^{2-} . SO_3^{2-} was not detected in any of these systems.

Surface Oxidation Products--

To measure the surface pyrite oxidation products, experiments were conducted with large pyrite particles both in the presence and absence of 1 mM CCl_4 . After 5 weeks of reaction at 25 °C, no measurable amount of CCl_4 had reacted, but after 5 more weeks of reaction at 50 °C, approximately 1 μM CCl_4 had reacted.

As shown in Figure 17, XPS analysis of the sulfur 2p peak does not show any effect on the near-surface of pyrite from reaction with 1 μM CCl_4 . The concentration of pyrite surface sites that had reacted with CCl_4 is estimated to be 10^{-4} - 10^{-5} mole/ m^2 which is too low to be detected using XPS. Using scanning tunneling microscopy (STM), early stages of oxidation of pyrite in air have been observed to occur at isolated spots or patches (C. Eggleston, EAWAG, Dübendorf, Switzerland, personal communication, 1993). Techniques such as in situ STM or atomic force

microscopy (AFM) may be more helpful to study surface oxidation of pyrite by CCl_4 in the future.

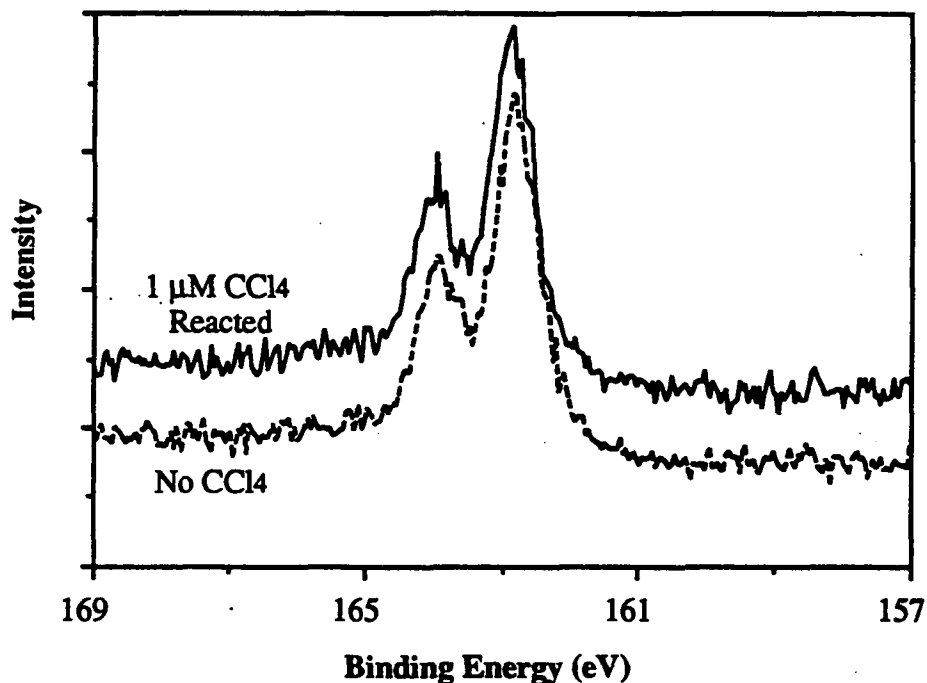


Figure 17: XPS spectra comparing S 2p peak for pyrite reacted under anaerobic conditions in the presence and absence of 1 μM CCl_4 .

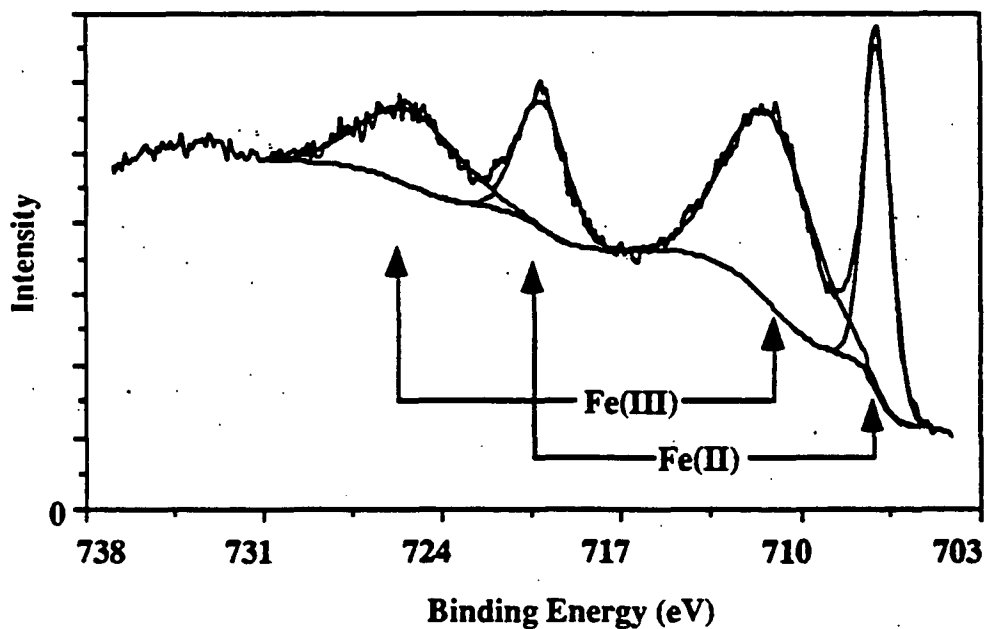


Figure 18: XPS spectra of Fe 2p peak of air-exposed pyrite reacted aerobically. The Fe(III) peaks are indicative of an iron oxide coating on the pyrite.

Oxidation of the near-surface of pyrite due to reaction under aerobic conditions was observed using XPS. The pyrite reacted aerobically for 5 and 10 weeks showed significant formation of an iron oxide at the surface.

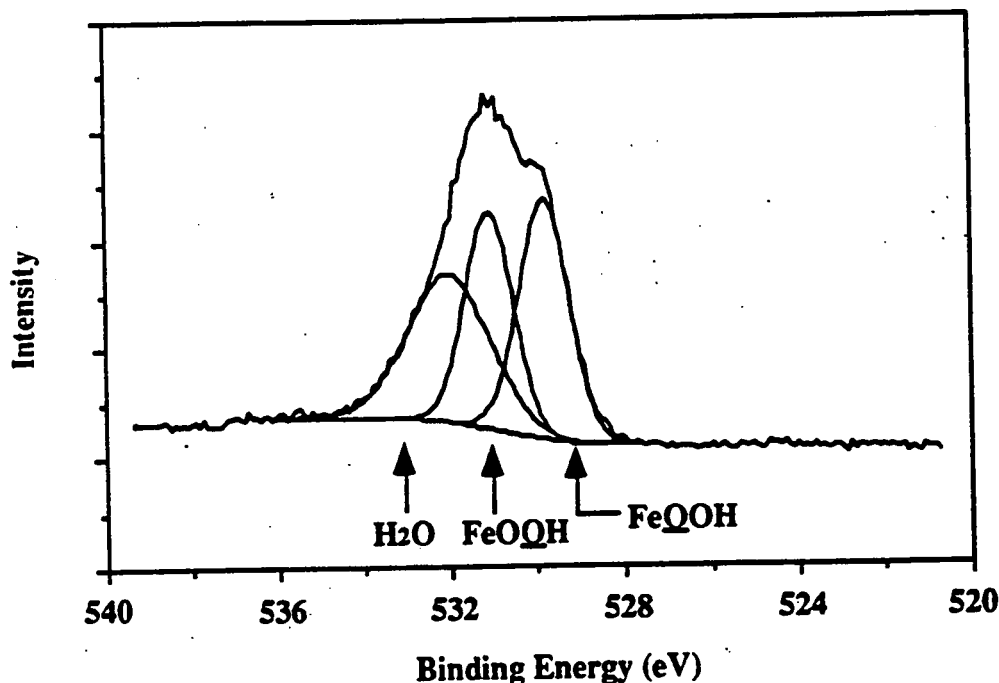


Figure 19: XPS spectra of O 1s peak of air-exposed pyrite reacted aerobically. The peaks at 530.1 and 531.2 eV coincide with the O 1s peak for FeOOH (Moulder et al., 1992).

The iron oxide is assumed to be FeOOH, as evidenced by the shape of the Fe 2p line (Figure 18) and the O 1s line (Figure 19) (Moulder et al., 1992). The peaks at 530.35 eV and 531.77 eV are the same size and width, within 5%. According to Moulder et al. (1992), the FeOOH and FeOOH peaks occur at 530.1 and 531.2 eV, respectively. Additionally, the ratio of FeOOH-Fe to FeOOH-O is 0.45 which is close to the expected ratio of 0.5. Goethite (α -FeOOH) and lepidocrocite (γ -FeOOH) cannot be distinguished using XPS. The O 1s peak in other iron hydroxides, such as Fe(OH)₃, would appear as one peak because the oxygens are in an identical environment. The O 1s peak for water is at 533.2 eV (Moulder et al., 1992), which likely corresponds to the broader peak at high binding energy (532.85 eV). The peak energies in Figure 19 do not correspond exactly to those in the literature, probably due to the electronic difference between pure FeOOH and an FeOOH coating on pyrite. The mechanism of formation of iron hydroxides on pyrite is proposed to occur via surface complexation of Fe(OH)_{3-n}ⁿ⁺ species on the pyrite surface that ultimately recrystallize to goethite (Fornasiero et al., 1992). Therefore it is assumed that the iron oxide coating formed on pyrite is goethite. There was not a significant difference in the sulfur peak (2p) from the air-exposed/aerobic samples compared with the fresh-ground pyrite reacted anaerobically (Figure 20). The sulfur peaks were mostly attributed to pyrite-sulfur (>90%) (Hyland and Bancroft, 1990; Szargen et al., 1992). Small shoulders observed on the low and high binding energy sides of the sulfur 2p peak can be attributed to FeS (Moulder et al., 1992) and partially oxidized sulfur, such as polysulfides and elemental sulfur (Hyland and Bancroft, 1990; Szargen et al., 1992), respectively. Small differences in these shoulders observed under distinct reaction conditions were too small to be quantified.

Under all reaction conditions, the near-surface of the pyrite was depleted in ferrous iron. The S:Fe(II) ratio was greater than 4 in all cases (Table 9), whereas it was 2.1 for fresh-cleaved pyrite. The depth of analysis using XPS decreases by the factor $(1 - e^{-n})$ where n is the number of the attenuation lengths of the photoelectron, (λ) . Therefore, 63% of the signal is within 1λ . Since $\lambda = 18 \text{ \AA}$ for the S 2p peak (Baltrus and Proctor, 1990), the depth of this leached layer is probably a several unit cells thick (5.4 \AA per unit cell). With more than one in two Fe^{2+} leached from the near surface of the pyrite lattice, a shift in the S 2p peak is expected. This shift would be evidenced as peak broadening of the S 2p due to contributions of both FeS_2 -S and leached S_2 -S. However, no significant differences were observed in the S 2p peak shape for fresh-cleaved pyrite and pyrite reacted in water for 10 weeks (data not shown). It appears that iron is being leached from the pyrite surface while the electronic structure of the sulfur is apparently unchanged.

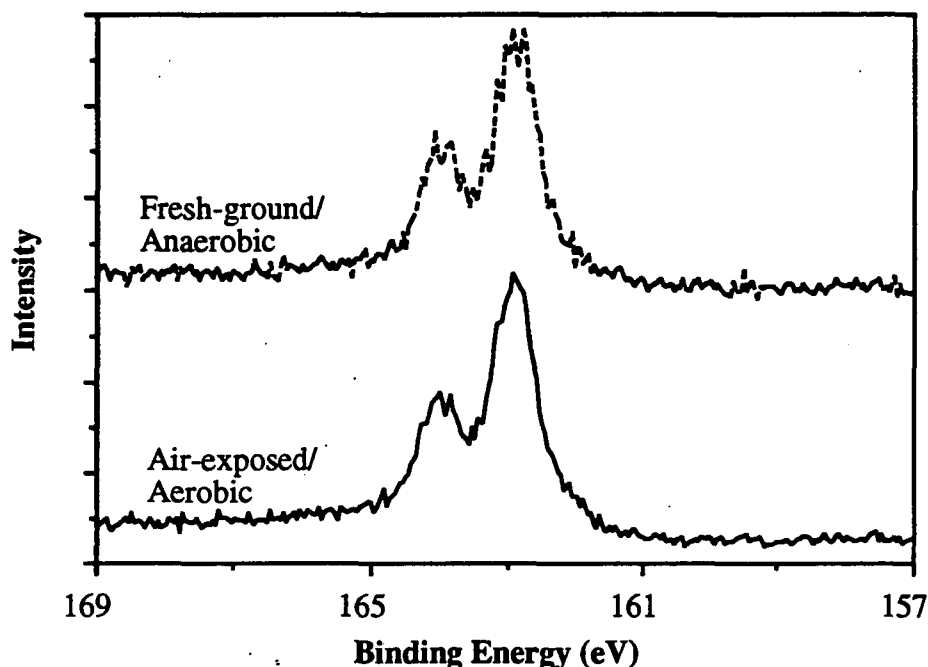


Figure 20: XPS spectra of the S 2p peak comparing fresh-ground pyrite reacted anaerobically with air-exposed pyrite reacted aerobically. There is no significant difference in the S 2p peak shapes and binding energies under these reaction conditions.

In experiments with sphalerite (ZnS) at pH 5-7, Rönngren et al. (1991) observed leaching of Zn^{2+} to solution, without a significant release of S. The appearance of Zn^{2+} in solution corresponded with a loss of two times the number protons from solution, suggesting a hydrolysis or ion exchange reaction of the form,



(Rönngren et al., 1991). Similarly, ion exchange of 2H^+ for Pb^{2+} was observed for galena (Sun et al., 1991). Although the solution chemistry was not quantified for pyrite, the XPS data intimate that a similar leaching reaction is occurring in these systems. The binding energy for S 2p in a species such as S_2H_2 is not known, however it is expected to be at higher binding energy because the nuclei of H_2^{2+} are less shielded than Fe^{2+} . Nonetheless, it is conceivable that the binding energy shift of S in H_2S_2 is less than the resolution of the instrument (0.8 eV), thus

explaining the lack of peak broadening in the S 2p peak. The effect of this leaching on the reactivity of the pyrite toward oxidation is unknown.

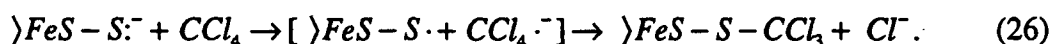
Table 9: Effect of environmental conditions on S:Fe(II) in the near-surface of pyrite where S:Fe(II) was determined using XPS.

Reaction Conditions	S:Fe(II)
Fresh-cleaved pyrite	2.1
Air-exposed pyrite, Aerobic ^a	4.6
Air-exposed pyrite, Sulfide ^a	6.7
Air-exposed pyrite, Anaerobic ^a	6.0
Fresh-ground pyrite, Anaerobic ^a	4.7
Acid-treated pyrite, Anaerobic ^a	4.8

^a After reaction in water for 10 weeks.

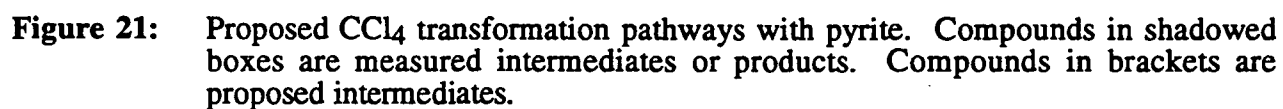
Proposed Mechanism at Pyrite Surface

Sulfur is the proposed electron transfer site in reactions of CCl₄ with pyrite because the surface was depleted in iron and CS₂ was detected under all reaction conditions. Since the pyrite surface was negatively charged under the reaction conditions in this study, the surface sites are proposed to be predominantly of the form, >FeSS⁻. It is assumed that the amphoteric nature of the leached pyrite surface is similar to that of pyrite-S. In the absence of oxidation of the pyrite surface, the reaction with CCl₄ is proposed to occur via the reaction,



It is unlikely that a concerted S_N2 reaction occurs between pyrite-S and CCl₄. Rather, a radical reaction is proposed above because of the resonance stability of the three-electron C-Cl bond in CCl₄⁻ (Shaik, 1983; Pross, 1985 a, b). An electron would be transferred from the π* orbital on the pyrite-sulfur to a σ* orbital in CCl₄. Since CCl₄ or an intermediate must react directly with the pyrite surface, formation of the proposed FeSSCCl₃ intermediate is plausible. Subsequent reaction of FeSSCCl₃ is uncertain, but speculation is summarized in Figure 21 and discussed below.

In the fresh-ground pyrite system, CHCl₃ is the major product. The reaction probably proceeds with an additional electron to form a trichloromethyl anion (:CCl₃⁻) which can react with a proton in solution to form CHCl₃. The pyrite-sulfur will be hydroxylated and subsequently oxidized until a sulfoxy species forms that is stable in solution. No sulfoxy species were detected on the pyrite surface using XPS, either because the concentrations were too low or the hydroxylation reactions are fast. As predicted in the above pathway, the sulfoxy species, S₂O₃²⁻, was detected in systems with extensive reaction by CCl₄.



The path to form CS₂ will depend on the strength of the S-S bond relative to the S-CCl₃ bond. As indicated in Figure 21, FeSSCCl₃ may react with OH⁻ to form FeSOH and ⁻SCCl₃ (trichloromethylthiolate) or FeOH and ⁻SSCCl₃ (trichloromethyldithiolate). Both the trichloromethyldithiolate and the trichloromethylthiolate may decompose in separate pathways to form thiophosgene (dichlorothionomethane) which may react again with another sulfide group at the pyrite surface to form CS₂. If a one-electron transfer is assumed as the initial step (Equation 26), the carbon in CCl₄ (+IV) is first reduced to form the transition state {Cl-CCl₃⁻ (+III)} followed by oxidation to form CS₂ (+IV). In this reaction scheme the disulfide group on pyrite undergoes a disproportionation reaction wherein one sulfur of the disulfide group is reduced to the -II state (CS₂) and one sulfur of the disulfide is oxidized to the 0 state (>FeSOH).

The path to form CO₂ can occur via hydrolysis of CS₂ or reaction of the trichloromethyl radical with O₂. The former pathway is assumed to prevail under anaerobic conditions. However, under aerobic conditions, CO₂ is the major product in the pyrite system and both pathways are possible. Although the modeling results were inconclusive, they were consistent with a pathway in which all the CO₂ is formed by hydrolysis of CS₂. The formation of CS₂ under these conditions was proposed to occur via a stable intermediate that is adsorbed to the surface. XPS data show significant formation of FeOOH on the pyrite surface. Goethite can influence the reaction of CCl₄ in several ways. Electron transfer can occur across the iron oxide coating because FeOOH is a semi-conductor. CCl₄ may be accepting an electron at the FeOOH/water interface to form Cl₃C[•]. The radical can then react with O₂ to form CO₂ or with pyrite-S to form CS₂. It seems unlikely that Cl₃C[•] would be formed at the oxide surface and then react with pyrite-S because the reaction rate of Cl₃C[•] with O₂ is close to the diffusion limit (Asmus et al., 1985). Lastly, CCl₄ may be reacting with pyrite-S to form an intermediate such as, ⁻SSCCl₃, that is stabilized at the FeOOH/water interface since the pH_{pzc} of goethite is 7.3-8.3 (Hingston et al., 1972; Sigg and Stumm, 1981). Although the data preclude determination of the pathway to form CO₂, it is clear that the presence of O₂ significantly affects the CCl₄ transformation pathway.

Summary of Pyrite Experiments

Pyrite was shown to be very reactive toward CCl₄. Under all environmental conditions studied, >90 % of 1 μM CCl₄ reacted within 12-36 days at 25 °C in the presence of 1.2-1.4 m²/L pyrite. Zeroth-order dependence on the CCl₄ concentration was observed, suggesting a surface-controlled reaction. The rates of transformation of CCl₄ under all conditions are fast enough such that oxidation of pyrite by CCl₄ should not be curtailed in the presence of competing oxidants, such as Fe³⁺ and O₂. The CCl₄ product distribution was very dependent on reaction conditions. Under aerobic conditions, CO₂ was the major transformation product; whereas in the fresh-ground pyrite system, CHCl₃ was the major product.

Although these laboratory rates of CCl₄ transformation by pyrite cannot yet be extrapolated to field conditions because of the confounding effects of natural organic matter, co-solvents, and competing oxidants, the reactivity under different environmental conditions can be compared qualitatively. In a sulfate reducing environment, the transformation rate of CCl₄ may be retarded by the presence of sulfide, whereas in the absence of aqueous sulfide; the fastest transformation rates would be expected. Under aerobic conditions, oxide coatings on pyrite will likely retard the transformation of CCl₄; but the transformation products are environmentally desirable.

REFERENCES

- Adewuyi, Y.G. and G.R. Carmichael (1987) Kinetics of hydrolysis and oxidation of carbon disulfide by hydrogen peroxide in alkaline medium and application to carbonyl sulfide, *Environ. Sci. Technol.*, 21: 170-177.
- Anderson, L.D., D.B. Kent, and J.A. Davis (1992) Batch experiments characterizing the reduction of Cr(VI) using suboxic material from a mildly reducing sand and gravel aquifer, *Abst. Am. Chem. Soc. Mtg.*, April 5-10, 1992, San Francisco, CA.
- Anderson, L.D., D.B. Kent, and J.A. Davis (1994) Batch experiments characterizing the reduction of Cr(VI) using suboxic material from a mildly reducing sand and gravel aquifer *Environ. Sci. Technol.*, in press.
- Asmus, K.D., D. Bahnemann, K. Krischer, M. Lal, and J. Mönig (1985) One-electron induced degradation of halogenated methanes and ethanes in oxygenated and anoxic aqueous solutions, *Life Chem. Rep.*, 3: 1-15.
- Baltrus, J.P. and A. Proctor (1990) Composition of overlayers on oxidized pyrite surfaces, *Appl. Surf. Sci.*, 44: 147-150.
- Barbash, J.E. and M. Reinhard (1989a) The Reactivity of Sulfur Nucleophiles Toward Halogenated Organic Compounds in Natural Waters, in *Biogenic Sulfur in the Environment*; E.S. Saltzman and W.J. Cooper, eds., ACS Symposium Series 393, American Chemical Society: Washington, D.C., pp 101-138.
- Barbash, J.E. and M. Reinhard (1989b) Abiotic dehalogenation of 1,2-dichloroethane and 1,2-dibromoethane in aqueous solution containing hydrogen sulfide, *Environ. Sci. Technol.*, 23: 1349-1358.
- Barber, L.B., II, E. M. Thurman, and D.D. Runnells (1992) Geochemical heterogeneity in a sand and gravel aquifer: Effect of sediment mineralogy and particle size on the sorption of chlorobenzenes, *J. Contam. Hydrol.*, 9: 35-54.
- Begheijn, L.Th. (1979) Determination of iron(II) in rock, soil, and clay, *Analyst*, 104: 1055-1061.
- Burneau, A. and O. Barres (1990) Comparative study of the surface hydroxyl groups of fumed and precipitated silicas. 2. Characterization by infrared spectroscopy of the interactions with water, *Langmuir*, 6: 1364-1372.
- Castro, C.E. and W.C. Kray, Jr. (1963) The cleavage of bonds by low valent transition metal ions. The homogeneous reduction of alkyl halides by chromous sulfate., *J. Am. Chem. Soc.*, 85: 2768-2773.
- Castro, C.E. and W. C. Kray, Jr. (1966) Carbenoid intermediates from polyhalomethanes and chromium(II). The homogeneous reduction of geminal halides by chromous sulfate., *J. Am. Chem. Soc.*, 88: 4447-4455.

- Criddle, C.S. and P.L. McCarty (1991) Electrolytic model system for reductive dehalogenation in aqueous environments, *Environ. Sci. Technol.*, 25: 973-978.
- Criddle, C.S., J.T. DeWitt, and P.L. McCarty (1990) Reductive dehalogenation of carbon tetrachloride by *Escherichia coli* K-12, *Appl. Environ. Microbiol.*, 56: 3247-3254.
- Criddle, C.S., P.L. McCarty, M.C. Elliott, and J.F. Barker (1986) Reduction of hexachloroethane to tetrachloroethylene in ground waterwater, *J. Contam. Hydrol.*, 1: 133-142.
- Curtis, G.P. (1991) Reductive dehalogenation of hexachloroethane and carbon tetrachloride by aquifer sand and humic acid., Ph.D. Dissertation, Department of Civil Engineering, Stanford University, Stanford, CA.
- Curtis, G.P. and M. Reinhard (1993) Reductive dehalogenation of hexachloroethane and carbon tetrachloride and bromoform by anthrahydroquinone disulfonate and humic acid (submitted *Environ. Sci. Technol.*, March, 1993).
- Davis, J. A. and J.D. Hem (1989) The surface chemistry of aluminum oxides and hydroxides, In *The Environmental Chemistry of Aluminum.*, (G. Sposito, ed.), Chapter 7, CRC Press, Inc., Boca Raton, FL.
- Deer, W.A., R.A. Howie, and J. Zussman (1982) *An Introduction to the Rock Forming Minerals*, Longman Group Limited, Essex, England.
- dos Santos Afonso, M. and W. Stumm (1992) The reductive dissolution of iron(III) (hydr)oxides by hydrogen sulfide, *Langmuir*, 8: 1671-1675.
- Fadrus, H. and J. Maly (1975) Suppression of iron(III) interference in the determination of iron(II) in water by the 1,10-phenanthroline method, *Analyst*, 100: 549-554.
- Fornasiero, D., V. Eijt, and J. Ralston (1992) An electrokinetic study of pyrite oxidation, *Colloids Surf.*, 62: 63-73.
- Fritz, S.F. and R.K. Popp (1985) A single-dissolution technique for determining FeO and Fe₂O₃ in rock and mineral samples, *Amer. Mineral.*, 70: 961-968.
- Goldhaber, M.B. (1983) Experimental study of metastable sulfur oxyanion formation during pyrite oxidation at pH 6-9 and 30 °C, *Amer. J. Sci.*, 283: 193-217.
- Haag, W. and T. Mill (1988) Some reactions of naturally occurring nucleophiles with haloalkanes in water, *Environ. Toxicol. Chem.*, 7: 917-924.
- Hileman, B. (1993) Concerns broaden over chlorine and chlorinated hydrocarbons, *Chem. Eng. News*, April 19, 1993, pp 11-20.
- Hingston, F.J., A.M. Posner, and J.P. Quirk (1972) Anion adsorption by goethite and gibbsite. I. The role of the proton in determining adsorption envelopes, *J. Soil Sci.*, 23: 177-192.
- Hovenkamp, S.G. (1963) Sodium dithiocarbonate as a by-product in xanthating reactions. A contribution to the chemistry of viscose, *J. Polymer Sci., Part C.*, No. 2, 341-355.

- Howarth, R.W. and J.M. Teal (1979) Sulfate reduction in a New England salt marsh, *Limnol. Oceanogr.*, 24: 999-1013.
- Huerta-Diaz, M.A. and J.W. Morse (1992) Pyritization of trace metals in anoxic marine sediments, *Geochim. Cosmochim. Acta*, 56: 2681-2702.
- Hyland, M.M. and G.M. Bancroft (1989) An XPS study of gold deposition at low temperatures on sulphide minerals: reducing agents, *Geochim. Cosmochim. Acta*, 52: 385-394.
- Hyland, M.M. and G.M. Bancroft (1990) Palladium sorption and reduction on sulphide mineral surfaces: An XPS and AES study, *Geochim. Cosmochim. Acta*, 54: 117-130.
- Jeffers, P.M., L.M. Ward, L.M. Woytowitch and N.L. Wolfe (1989) Homogeneous hydrolysis rate constants for selected chlorinated methanes, ethanes, ethenes, and propanes, *Environ. Sci. Technol.*, 23: 965-969.
- Katser, R.P. and V.M. Ropot (1986) A study of hydrosulfide ion sorption on natural sorbents, *Khim. Tekhnol. Vody*, 8: 81-82.
- Knauss, K.G. and T.J. Wolery (1989) Muscovite dissolution kinetics as a function of pH and time at 70 °C, *Geochim. Cosmochim. Acta*, 53: 1493-1501.
- Kreyszig, E. (1983) *Advanced Engineering Mathematics*, 5th ed., J. Wiley & Sons, New York.
- Kriegman-King, M.R. (1993) Abiotic transformation of carbon tetrachloride at mineral surfaces, Ph.D. Dissertation, Department of Civil Engineering, Stanford University, Stanford, CA.
- Kriegman-King, M.R. and M. Reinhard (1991) Reduction of hexachloroethane and carbon tetrachloride at surfaces of biotite, vermiculite, pyrite and marcasite, In *Organic Substances and Sediments in Water* (R.A. Baker, ed.) Vol II, Lewis Publishers, Chelsea, MI, pp 349-364.
- Kriegman-King, M.R. and M. Reinhard (1992) Transformation of carbon tetrachloride in the presence of sulfide, biotite, and vermiculite, *Environ. Sci. Technol.*, 26: 2198-2206.
- Lasaga, A.C. (1981) Rate laws of chemical reactions, In *Kinetics of Geochemical Processes*, (A.C. Lasaga, ed.), Reviews in Mineralogy, Vol 8, Mineralogical Society of America, Washington, D.C., pp 1-68.
- Lasaga, A.C. (1984) Chemical kinetics of water-rock interactions, *J. Geophys. Res.*, 89: 4009-4025.
- Lord, C.J., III and T.M. Church (1983) The geochemistry of salt marshes: Sedimentary ion diffusion, sulfate reduction, and pyritization, *Geochim. Cosmochim. Acta*, 47: 1381-1391.
- Luther, G.W., III (1990) The frontier-molecular-orbital theory approach in geochemical processes, In *Aquatic Chemical Kinetics*, (W. Stumm, ed.), Wiley Interscience, New York, pp 173-198.
- Luther, G.W., III, A. Giblin, R.W. Howarth, and R.A. Ryans (1982) Pyrite and oxidized iron mineral phases formed from pyrite oxidation in salt marsh and estuarine sediments, *Geochim. Cosmochim. Acta*, 46: 2665-2669.

- Macalady, D.L., P.G. Tratnyek, and T.J. Grundl (1986) Abiotic reduction reactions of anthropogenic organic chemicals in anaerobic systems: a critical review, *J. Contam. Hydrol.*, 1: 1-28.
- McKibben, M.A. and H.L. Barnes (1986) Oxidation of pyrite in low temperature acidic solutions: rate laws and surface textures, *Geochim. Cosmochim. Acta*, 50: 1509-1520.
- Millero, F.J. (1986) The thermodynamics and kinetics of the hydrogen sulfide system in natural waters, *Mar. Chem.*, 18: 121-147.
- Moses, C.O., D.K. Nordstrom, J.S. Herman, and A.L. Mills (1987) Aqueous pyrite oxidation by dissolved oxygen and by ferric iron, *Geochim. Cosmochim. Acta*, 51: 1561-1571.
- Moses, C.O. and J.S. Herman (1991) Pyrite oxidation at circumneutral pH, *Geochim. Cosmochim. Acta*, 55: 471-482.
- Moulder, J.F., W.F. Stickle, P.E. Sobol, and K.D. Bomben (1992) *Handbook of X-ray Photoelectron Spectroscopy* (J. Chastain, ed.), Perkin-Elmer Corporation, Eden Prairie, MN.
- Mycroft, J.R., G.M. Bancroft, N.S. McIntyre, J.W. Lorimer, and I.R. Hill (1990) Detection of sulphur and polysulfides on electrochemically oxidized surfaces by X-ray photoelectron spectroscopy and Raman spectroscopy, *J. Electroanal. Chem. and Interfacial. Electrochem.*, 292: 139-152.
- Nicholson, R.V., R.W. Gillham, and E.J. Reardon (1988) Pyrite oxidation in carbonate-buffered solution: 1. Experimental kinetics, *Geochim. Cosmochim. Acta*, 52: 1077-1085.
- Nicholson, R.V., R.W. Gillham, and E.J. Reardon (1990) Pyrite oxidation in carbonate-buffered solution: 2. Rate control by oxide coatings, *Geochim. Cosmochim. Acta*, 54: 395-402.
- Papirer, E., J.M. Perrin, B. Siffert, G. Philipponneau, and J.M. Lamerant (1993) The influence of grinding on the surface properties of α -aluminas, *J. Coll. Int. Sci.* 156: 104-108.
- Peiffer, S., M. dos Santos Afonso, B. Wehrli, and R. Gächter (1992) Kinetics and mechanism of the reaction of H_2S with lepidocrocite, *Environ. Sci. Technol.*, 26: 2408-2413.
- Pross, A. (1985a) A general approach to organic reactivity: The configuration mixing model, In *Advances in Physical Organic Chemistry*, (V. Gold and D. Bethell, eds.), Academic Press, San Diego, pp 99-196.
- Pross, A. (1985b) The single electron shift as a fundamental process in organic chemistry: The relationship between polar and electron transfer pathways, *Acc. Chem. Res.*, 18: 212-219.
- Pyzik, A.J. and S.E. Sommer (1981) Sedimentary iron monosulfides: Kinetics and mechanism of formation, *Geochim. Cosmochim. Acta*, 45: 687-698.
- Rönngren, L., S. Sjöberg, Z. Sun, W. Forsling, and P.W. Schindler (1991) Surface reactions in aqueous metal sulfide systems. 2. Ion exchange and acid/base reactions at the $ZnS-H_2O$ interface, *J. Coll. Int. Sci.*, 145: 396-404.

- Rowland, F.S. (1991) Stratospheric ozone in the 21st century: The chlorofluorocarbon problem, *Environ. Sci. Technol.*, 25: 622-628.
- Sax, N.L. and R.J. Lewis, Sr. (1987) *Hazardous Chemicals Desk Reference*, Van Nostrand Reinhold Co., New York, pp 299-300.
- Schwarzenbach, R.P. and P.M. Gschwend (1990) Chemical transformations of organic pollutants in the aquatic environment, In *Aquatic Chemical Kinetics*, (W. Stumm, ed.), J. Wiley & Sons, New York, 199-233.
- Scofield, J.H. (1976) Hartree-Slater subshell photoionization cross-sections at 1254 and 1487 eV, *J. Elec. Spectr. Rel. Phen.*, 8: 129-137.
- Shaik, S.S. (1983) α - and β -carbon substituent effect on S_N2 reactivity. A valence-bond approach, *J. Am. Chem. Soc.*, 105: 4359-4367.
- Sigg, L. and W. Stumm (1981) The interaction of anions and weak acids with the hydrous goethite (α -FeOOH) surface, *Colloids and Surfaces*, 2: 101-117.
- Singer, P.C. and W. Stumm (1970) Acid mine drainage--The rate limiting step, *Science*, 167: 1121-1123.
- Sposito, G. (1989) *The Chemistry of Soils*, Oxford University Press, New York.
- Stone, A. and J.J. Morgan (1987) Reductive dissolution of metal oxides, In *Aquatic Surface Chemistry*, (W. Stumm, ed.), J. Wiley & Sons, New York, 221-254.
- Stumm, W. and J.J. Morgan (1981) *Aquatic Chemistry*, J. Wiley and Sons, New York, p 456.
- Sun, Z., W. Forsling, L. Rönngren, S. Sjöberg and P.W. Schindler (1991) Surface reactions in aqueous metal sulfide systems. 3. Ion exchange and acid/base properties of hydrous lead sulfide, *Colloids. Surf.*, 59: 243-254.
- Swain, C.G. and C.B. Scott (1953) Quantitative correlation of relative rates. Comparison of hydroxide ion with other nucleophilic reagents toward alkyl halides, esters, epoxides, and acyl halides., *J. Am. Chem. Soc.*, 75: 141-147.
- Swider, K.T. and J.E. Mackin (1989) Transformations of sulfur compounds in marsh-flat sediments, *Geochim. Cosmochim. Acta*, 53: 2311-2323.
- Szargan, R., S. Karthe, and E. Suoninen (1992) XPS studies of xanthate adsorption on pyrite, *Appl. Surf. Sci.*, 55: 227-232.
- Taylor, B.E., M.C. Wheeler, and D.K. Nordstrom (1984) Stable isotope geochemistry of acid mine drainage: experimental oxidation of pyrite, *Geochim. Cosmochim. Acta*, 48: 2669-2678.
- Tchobanoglous, G. and E.D. Schroeder (1985) *Water Quality*, Addison-Wesley Publishing Co., Menlo Park, CA.
- Umaña, A.F. (1979) Kinetics of oxidative dissolution of pyrite by aqueous chlorine species, Ph.D. Dissertation, Department of Civil Engineering, Stanford University, Stanford, CA.

- Vairavamurthy, A. and K. Mopper (1989) Mechanistic studies of organosulfur (thiol) formation in coastal marine sediments, In *Biogenic Sulfur in the Environment*, (E.S. Saltzman and W.J. Cooper, eds.), ACS Symposium Series 393, American Chemical Society, Washington, D.C., pp 231-242.
- White, A.F. and A. Yee (1985) Aqueous oxidation-reduction kinetics associated with coupled electron-cation transfer from iron-containing silicates at 25 °C, *Geochim. Cosmochim. Acta*, 49: 1263-1275.
- White, G.N., J.B. Dixon, R.M. Weaver, and A.C. Kunkle (1991) Genesis and morphology of iron sulfides in gray kaolins, *Clays Clay Min.*, 39: 70-76.
- Wieland, E., B. Wehrli, and W. Stumm (1988) The coordination chemistry of weathering: III. A generalization on the dissolution rates of minerals, *Geochim. Cosmochim. Acta*, 52: 1969-1981.
- Wiersma, C.L. and J.D. Rimstidt (1984) Rates of reaction of pyrite and marcasite with ferric iron at pH 2, *Geochim. Cosmochim. Acta*, 48: 85-92.

NTIS does not permit return of items for credit or refund. A replacement will be provided if an error is made in filling your order, if the item was received in damaged condition, or if the item is defective.